Title

Protein Tyrosine Phosphatase 1B Regulates Pyruvate Kinase M2 Tyrosine Phosphorylation*

Journal

Journal of Biological Chemistry, 288(24)

ISSN

0021-9258

Authors

Bettaieb, Ahmed
Bakke, Jesse
Nagata, Naoto
et al.

Publication Date

2013-06-01

DOI

10.1074/jbc.m112.441469

Peer reviewed

THE JOURNAL OF BIOLOGICAL CHEMISTRY VOL. 288, NO. 24, pp. 17360–17371, June 14, 2013

Protein Tyrosine Phosphatase 1B Regulates Pyruvate Kinase M2 Tyrosine Phosphorylation*[S]

Received for publication, December 3, 2012, and in revised form, April 24, 2013 Published, JBC Papers in Press, May 2, 2013, DOI 10.1074/jbc.M112.441469

Ahmed Bettaieb[‡1], Jesse Bakke[‡1], Naoto Nagata[‡], Kosuke Matsuo[‡], Yannan Xi[‡], Siming Liu[‡], Daniel AbouBechara[‡], Ramzi Melhem[‡], Kimber Stanhope[‡§], Bethany Cummings[‡§], James Graham[‡§], Andrew Bremer[¶], Sheng Zhang[‖], Costas A. Lyssiotis[‡‡2], Zhong-Yin Zhang[‖], Lewis C. Cantley[**‡‡2], Peter J. Havel[‡§], and Fawaz G. Haj[‡§§¶¶3]**

*From the [‡]Nutrition Department and [§]Department of Molecular Biosciences, University of California Davis, Davis, California 95616, the [¶]Department of Pediatrics, Vanderbilt University, Nashville, Tennessee 37232, the [‖]Department of Biochemistry and Molecular Biology, Indiana University, Indianapolis, Indiana 46202, the **Beth Israel Deaconess Medical Center, Department of Medicine, and [‡‡]Department of Systems Biology, Harvard Medical School, Boston, Massachusetts 02115, and the [§§]Department of Internal Medicine and [¶¶]Comprehensive Cancer Center, University of California Davis, Sacramento, California 95817*

Background: Tyrosine phosphorylation of PKM2 inhibits its activity; however, the phosphatase(s) that regulates PKM2 phosphorylation remains unidentified.
Results: PKM2 is a novel PTP1B substrate and PKM2 Tyr-105 and Tyr-148 are key sites that mediate the interaction.
Conclusion: PTP1B regulates PKM2 tyrosine phosphorylation and activity in adipocytes.
Significance: These findings provide new insights into the regulation of adipose PKM2 activity.

Protein-tyrosine phosphatase 1B (PTP1B) is a physiological regulator of glucose homeostasis and adiposity and is a drug target for the treatment of obesity and diabetes. Here we identify pyruvate kinase M2 (PKM2) as a novel PTP1B substrate in adipocytes. PTP1B deficiency leads to increased PKM2 total tyrosine and Tyr[105] phosphorylation in cultured adipocytes and *in vivo*. Substrate trapping and mutagenesis studies identify PKM2 Tyr-105 and Tyr-148 as key sites that mediate PTP1B-PKM2 interaction. In addition, *in vitro* analyses illustrate a direct effect of Tyr-105 phosphorylation on PKM2 activity in adipocytes. Importantly, PTP1B pharmacological inhibition increased PKM2 Tyr-105 phosphorylation and decreased PKM2 activity. Moreover, PKM2 Tyr-105 phosphorylation is regulated nutritionally, decreasing in adipose tissue depots after high-fat feeding. Further, decreased PKM2 Tyr-105 phosphorylation correlates with the development of glucose intolerance and insulin resistance in rodents, non-human primates, and humans. Together, these findings identify PKM2 as a novel substrate of PTP1B and provide new insights into the regulation of adipose PKM2 activity.

The obesity epidemic and its associated comorbidities, including type 2 diabetes, cardiovascular disease, and many cancers, have increased interest in adipose tissue metabolism because this may present a novel therapeutic target (1). The adipose tissue integrates an array of homeostatic processes and is an important regulator of systemic insulin sensitivity and energy metabolism (2). There are two major types of adipose tissues in mammals: white and brown. White adipose tissue is the primary site for triglyceride storage or fatty acid release, whereas brown adipose tissue (BAT)[4] is a thermogenic tissue with an established role in the defense against cold and emerging antiobesity properties (3, 4). Genetic and molecular studies identify tyrosine phosphorylation as a regulator of adipose tissue function, systemic glucose homeostasis, and energy balance (5–9).

Tyrosine phosphorylation is tightly controlled by the opposing actions of protein tyrosine kinases and protein tyrosine phosphatases (PTPs) (10). Protein tyrosine phosphatase 1B (PTP1B) is a ubiquitously expressed non-receptor tyrosine-specific phosphatase that is localized on the cytoplasmic face of the endoplasmic reticulum (11–13). PTP1B is a physiological regulator of glucose homeostasis and energy balance. Specifically, whole-body PTP1B KO mice are hypersensitive to insulin, lean, and resistant to high-fat diet (HFD)-induced obesity (14, 15). Mice with tissue-specific PTP1B deletion in the liver and muscle exhibit improved glucose homeostasis independent of body weight (16–18), whereas mice with neuronal deletion exhibit decreased body weight (19). However, the role of PTP1B in adipocytes is unresolved, with studies demonstrating detri-

* This work was supported, in whole or in part, by National Institutes of Health Grants R56DK084317 and R01DK090492 (to F. G. H.); AT-003645, HL-075675, HL-091333, and DK-087307 (to P. J. H.); CA-69202 (to Z. Y. Z.); and NCI and National Institutes of Health grants (to L. C. C.). This work was also supported by Juvenile Diabetes Research Foundation Research Grant 1-2009-337) (to F. G. H.), by a Training Program in Biomolecular Technology Fellowship T32-GM008799 (to J. B.), by an American Diastases Association and multicampus award from the University of California, Office of the President (to P. J. H.), and by Damon Runyon Cancer Research Foundation Amgen Fellowship DRG-2056-10 (to C. A. L.). Dr. Cantley owns equity in and receives compensation from Agios Pharmaceuticals and serves on the Board of Directors and Scientific Advisory Board of Agios Pharmaceuticals. Agios Pharmaceuticals is identifying metabolic pathways of cancer cells and developing drugs to inhibit such enzymes to disrupt tumor cell growth and survival.
[S] This article contains supplemental Figs. S1–S4.
[1] Both authors contributed equally to this work.
[2] Present address: Department of Medicine, Cornell Weill Medical College, New York, NY 10065.
[3] To whom correspondence should be addressed: University of California Davis, Nutrition Department, 3135 Meyer Hall, Davis, CA 95616. Tel: 530-752-3214; Fax: 530-752-8966; E-mail: fghaj@ucdavis.edu.

[4] The abbreviations used are: BAT, brown adipose tissue; PTP, protein tyrosine phosphatase; PKM2; pyruvate kinase M2; HFD; high-fat diet; CII, compound II; D/A, PTP1B mutant D181A; IR; insulin receptor.

mental or beneficial effects of adipose PTP1B deficiency on body mass and insulin sensitivity (19, 20). Notably, PTP1B is a modulator of brown fat adipogenesis through a peroxisome proliferator-activated receptor γ-dependent mechanism, and PTP1B deficiency regulates PKR-like endoplasmic reticulum-regulated kinase phosphorylation and protein synthesis (21–23). Collectively, the salutary effects of PTP1B deficiency on obesity and diabetes have focused attention on it as a potential therapeutic target.

Pyruvate kinase (PK), a rate-limiting glycolytic enzyme, catalyzes the generation of pyruvate and ATP from phosphoenolpyruvate and ADP (24). In mammals, four pyruvate kinase isoforms exist: the L and R isoforms of the PKLR gene are expressed in liver and erythrocytes, respectively; the M1 splice isoform of the PKM gene is characteristic of more differentiated adult cells (*e.g.* muscle and brain); and the M2 isoform is expressed during embryonic development and in proliferative adult cell types (25). PKM2 expression facilitates aerobic glycolysis in tumors and provides a growth advantage (26, 27). Of note, tyrosine phosphorylation inhibits PKM2 activity (28). However, the phosphatase(s) that regulate(s) PKM2 remain(s) unidentified. In this study, we identify PKM2 as a novel PTP1B substrate and provide new insights into the regulation of adipose PKM2 activity.

EXPERIMENTAL PROCEDURES

Reagents—DMEM, G418, penicillin/streptomycin, puromycin, newborn calf serum, FBS, and trypsin were purchased from Invitrogen. PTP1B pharmacological inhibitor (compound II, CII) was prepared as described (29). Antibodies for human PTP1B (FG6), mouse PTP1B, and PKM1/2 were purchased from Abcam (Cambridge, MA). Tubulin antibodies were purchased from Upstate Biotechnology (Lake Placid, NY). PKM1 antibodies were purchased from Sigma. pPKM2 (Tyr-105), PKM2, pAKT (Ser-473), AKT, and FLAG antibodies were purchased from Cell Signaling Technology (Beverly, MA). pIR (Tyr-1162/Tyr-1163), and IR antibodies were purchased from Santa Cruz Biotechnology (Santa Cruz, CA). HRP-conjugated secondary antibodies were purchased from BioResources International (Carlsbad, CA). Unless indicated otherwise, chemicals were purchased from Sigma.

Cell Culture—Brown adipose cell lines were generated from whole-body PTP1B KO mice and reconstituted with human PTP1B WT and substrate-trapping mutant (D181A) as described previously (21). 3T3-L1 cells were maintained in DMEM containing 25 mM glucose, 10% newborn calf serum, 50 units/ml penicillin, and 50 μg/ml streptomycin. PKM silencing in 3T3-L1 cells was achieved by testing three different hairpins (Open Biosystems). Because the hairpins target regions that are shared for mouse PKM1 and PKM2, expression of both proteins was evaluated with one shRNA yielding a significant decrease in PKM2 without significant alterations in PKM1. Packaging (psPAX2) and envelope (pMD2.G) vectors were obtained from Addgene (Boston, MA). Lentiviruses were generated by cotransfection of vectors in HEK293FT cells using Lipofectamine 2000 (Invitrogen) following the guidelines of the manufacturer and then used to infect 3T3-L1 cells. Cells were selected using puromycin (2 μg/ml), and drug-resistant pools were propagated. Knockdown cells were reconstituted by transient transfection of PKM2 WT or mutants. Stable cell lines were selected using G418 at a concentration of 400 μg/ml.

To induce cell differentiation, brown and 3T3-L1 preadipocytes were grown to confluence in culture medium containing 10% FBS or 10% newborn calf serum, respectively. Confluent cells were then switched to differentiation medium containing 20% FBS, 20 nM insulin, and 1 nM triiodothyronine (T3) for 48 h. Adipocyte differentiation was induced by incubating cells for 48 h in differentiation medium further supplemented with 5 μM dexamethasone, 0.5 mM isobutylmethylxanthine, and 0.125 mM indomethacin (induction medium). After induction, cells were cultured in differentiation medium until they exhibited a differentiated phenotype with accumulation of fat droplets. For confocal microscopy, cells were grown on coverslips and fixed with 100% ice-cold methanol for 10 min and then blocked with 3% BSA in PBS for 60 min. After incubation with primary antibodies and fluorescent-conjugated secondary antibodies, cells were mounted in Mowiol (Sigma) and examined using Olympus FluoView laser-scanning confocal microscopy. Adipose tissue from different fat pads were fixed in 10% formalin and embedded in paraffin. Sections were stained using PKM2 and pPKM2 (Tyr-105) antibodies. Detection of protein specific bands was performed with appropriate fluorescein-conjugated secondary antibodies and visualized using a Leica DMI3000B inverted microscope.

Biochemical Analyses—Tissues/cells were homogenized in radioimmunoprecipitation assay buffer. Lysates were clarified by centrifugation at 13,000 rpm for 10 min, and protein concentrations were determined using a bicinchoninic acid assay kit (Pierce Chemical). Proteins (30–90 μg) were resolved by SDS-PAGE and transferred to PVDF membranes. For substrate-trapping experiments, cells were lysed in 1% Nonidet P-40 buffer with a protease inhibitor mixture (without sodium orthovanadate). Immune complexes were collected on PureProteome beads (Millipore) and washed with lysis buffer. Immunoblotting of lysates was performed with primary antibodies, and after incubation with secondary antibodies, proteins were visualized using enhanced chemiluminescence (Amersham Biosciences). Pixel intensities of immunoreactive bands were quantified using FluorChem Q imaging software (Alpha Innotech).

For site-directed mutagenesis, the indicated tyrosine (Y) to phenylalanine (F) mutations in mouse PKM2 cDNA were generated using a QuikChange Lightning site-directed mutagenesis kit (Agilent) following the instructions of the manufacturer and confirmed by DNA sequence analysis.

PTP1B Enzymatic Activity—3T3-L1 preadipocytes were treated with PTP1B inhibitor (compound II, 200 nM) (29) for 12 h and then lysed in Nonidet P-40 buffer (10 mM Tris-HCl (pH 7.4), 150 mM NaCl, 1 mM EDTA, 1% Nonidet P-40, 5% glycerol, and proteases inhibitors). 1 mg of total protein lysates was used to immunoprecipitate PTP1B using PureProteome beads (Millipore). The precipitate was washed twice with ice-cold lysis buffer and then resuspended in 50 μl of reaction buffer (50 mM HEPES (pH 5.0), 1 mM EDTA, 100 mM NaCl and 5 mM DTT) for 10 min, and the reaction was initiated by the addition of p-nitrophenyl phosphate (5 mM). PTP1B activity

was monitored by measuring the absorbance of p-nitrophenyl phosphate at 405 nm using a Wallac Victor 2 plate reader (PerkinElmer Life Sciences, Waltham, MA).

Measurement of Total Pyruvate Kinase Activity—Cells were lysed in 10 mM Tris-HCl (pH 7.5), 1.5 mM $MgCl_2$, 20 mM NaCl, 1 mM DTT, 1 mM PMSF, and a protease inhibitor mixture, incubated on ice for 20 min, and lysed with a glass Dounce homogenizer. Cell debris and unbroken cells were removed by centrifugation at 10,000 rpm for 15 min, and total pyruvate kinase activity was measured in the supernatant by a lactate dehydrogenase-coupled assay as described previously (30) with modifications. Briefly, proteins (1 μg) were added to 200 μl of reaction buffer containing 100 mM Tris-HCl (pH 8.0), 100 mM KCl, 10 mM $MgCl_2$, 0.5 mM EDTA, 0.2 mM β-NADH, 1.5 mM ADP, 5 mM phosphoenolpyruvate, and 0.6 units/ml lactate dehydrogenase. Pyruvate kinase activity was calculated at 25 °C by monitoring the absorbance at 340 nm using a Wallac Victor 2 plate reader. To determine the effects of PTP1B inhibition on pyruvate kinase activity cells were pretreated with CII for 12 h, and then pyruvate kinase activity was determined as described. CII was added to the lysis and reaction buffers.

LC-MS/MS Mass Spectrometry—Brown preadipocytes were cultured and differentiated as indicated. Adipocytes were homogenized in Nonidet P-40 buffer (10 mM Tris-HCl (pH 7.4), 150 mM NaCl, 1% IGEPAL^{TM} CA-630, and protease inhibitors). Lysates were clarified by centrifugation at 13,000 rpm for 10 min, and protein concentrations were determined using a bicinchoninic acid assay kit (Pierce Chemical). Proteins were resolved by SDS-PAGE, and gels were stained using Coomassie Brilliant Blue. Then, the 60- and 160-kDa bands were excised and processed by in-gel trypsin digestion to generate tryptic peptides. Tryptic peptides were resolved by reverse-phase chromatography (Cys-18) on an integrated nano-LC system (Easy-nLC, Proxeon Biosystems) and analyzed on a Linear Quadrupole ION Trap/Finnigan Polaris Q Mass Spectrometer (Thermo Scientific). Tandem mass spectra were extracted using ReadW.exe in centroid mode and searched with X!Tandem using the international protein index. Scaffold (Proteome Software) was used to validate MS/MS-based peptide and protein identifications as described previously (31).

Mouse Studies—C57Bl/6J (The Jackson Laboratory) male mice were maintained on a 12-hour light-dark cycle and fed *ad libitum*. Mice were fed standard lab chow (Purina Lab Chow, catalog no. 5001) or switched to a HFD (60% kcal from fat, catalog no. D12492, Research Diets) at 7 weeks of age. PTP1B-floxed (PTP1B fl/fl) mice were generated previously (19). Adiponectin-Cre mice were obtained from Dr. E. Rosen (Beth Israel Deaconess Medical Center/Harvard University). Genotyping for the PTP1B floxed allele and presence of Cre was performed by PCR using DNA extracted from tails as described (19). At the indicated age, mice were sacrificed, and different adipose depots were collected, frozen in liquid nitrogen, and then stored at −80 °C. Mouse studies were approved by Institutional Animal Care and Use Committee at the University of California Davis.

Human and Non-human Primate Studies—Rhesus monkeys (9–17 years old) provided by the California National Primate Research Center were maintained at the California National Primate Research Center at the University of California Davis. Monkeys were provided 500 ml/day of a fruit-flavored (Kool-Aid, Kraft Foods, Northfield, IL), 15% fructose-sweetened beverage (75 g of fructose) for 6 months or fed fructose supplemented with fish oil (fish oil, 4 g/day: 18% eicosapentaenoic acid and 12% docosahexaenoic acid Omega-3) for 6 months. Human subjects (40–72 years, body mass index 25–35 kg/m^2) were recruited for a 12-week study on the basis of the following exclusion criteria: evidence of diabetes, renal or hepatic disease, fasting serum triglyceride concentrations $>$ 400 mg/dl, blood pressure $>$ 140/90mmHg, and surgery for weight loss. Subjects consumed diets designed to maintain energy balance providing 15% of energy as protein, 30% as fat, and 55% as carbohydrate. Daily energy intake was calculated at base line using the Mifflin equation to estimate resting energy expenditure and adjusted for activity using a multiplication factor of 1.5. For the first 2-week inpatient base-line period, the carbohydrate content consisted primarily of complex carbohydrates and contained 8.8 $\pm$ 1.2 g of dietary fiber/1000 kcal. During the following 8 outpatient weeks of the study, subjects lived at home and consumed glucose or fructose beverages with their usual *ad libitum* diets. For the final 2-week inpatient intervention period, subjects consumed diets at the base-line energy level and macronutrient composition, except that 30% of the energy was from complex carbohydrates and 25% was provided by fructose- or glucose-sweetened beverages. The study was approved by the University of California Davis Institutional Review Board, and subjects provided informed consent to participate.

Statistical Analyses—Data are expressed as means $\pm$ S.E. Statistical analyses were performed using the JMP program (SAS Institute). Comparisons between groups were performed using unpaired two-tailed Student's *t* test. *, $p \leq 0.05$; **, $p \leq 0.01$.

RESULTS

Identification of Adipose PTP1B Substrates—To gain insight into the molecular mechanisms underlying PTP1B action, we utilized substrate-trapping and mass spectroscopy approaches to identify novel adipose PTP1B substrates. PTP1B WT has a high catalytic constant (32), rendering its interaction with substrates transient and difficult to detect. However, the steady-state interaction of PTP1B with its substrates is enhanced in the substrate-trapping PTP1B mutant D181A (D/A) that retains substrate binding but is catalytically impaired (33). Thus, PTP1B D/A forms stable complexes with tyrosine-phosphorylated substrates. The substrate-trapping approach has been utilized successfully to identify PTP1B substrates (13, 22, 33–35). Brown preadipocyte cell lines were generated from PTP1B KO mice and reconstituted with PTP1B D/A as described previously (21). PTP1B was immunoprecipitated from starved or insulin-stimulated (10 and 30 min) PTP1B D/A adipocytes, resolved using SDS-PAGE, and then immunoblotted with anti-phosphotyrosine antibodies. Upon insulin stimulation, two prominent hyperphosphorylated bands at ~60 and ~160 kDa were detected corresponding to "trapped" putative PTP1B substrates (Fig. 1*A*, *arrowheads*). Lysis under stringent conditions (radioimmunoprecipitation assay buffer) significantly attenuated tyrosine phosphorylation, likely because of disruption of PTP1B D/A-substrates coassociation. Proteins were stained

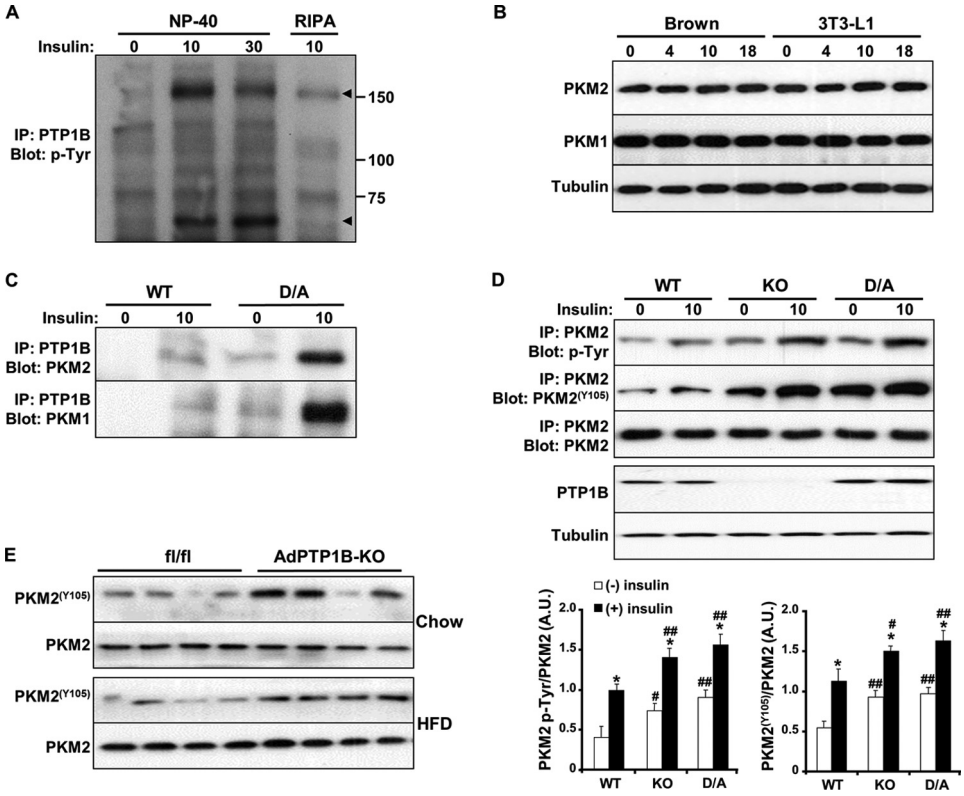

FIGURE 1. **Pyruvate kinase is a PTP1B substrate.** *A*, immunoblot analyses (*Blot*) of phosphotyrosine proteins in PTP1B immunoprecipitates from PTP1B D/A adipocytes starved or stimulated with insulin for 10 and 30 min. Cells were lysed in Nonidet P-40 or radioimmunoprecipitation assay buffer (*RIPA*), and PTP1B was immunoprecipitated (*IP*) using anti-human PTP1B antibodies (FG6) and immunoblotted using antibodies for phosphotyrosine. *Arrowheads* indicate hyperphosphorylated proteins. *B*, immunoblot analyses of PKM2, PKM1, and tubulin in lysates of brown and 3T3-L1 adipocytes at days 0, 4, 10, and 18 of differentiation. *C*, PTP1B was immunoprecipitated using FG6 antibodies from starved and insulin-stimulated PTP1B WT and D/A adipocytes (lysed in Nonidet P-40) and then immunoblotted using antibodies for PKM2 and PKM1. *D*, PKM2 was immunoprecipitated from lysates of PTP1B KO adipocytes and KO adipocytes reconstituted with PTP1B WT or PTP1B D/A and then immunoblotted using antibodies for phosphotyrosine, PKM2 (Tyr-105), and PKM2. Total cell lysates were blotted for PTP1B and tubulin. The *bar graph* represents normalized data for pTyr/PKM2 and PKM2 (Tyr-105)/PKM2, and data are presented as means ± S.E. *, significant difference between basal and insulin-stimulated conditions for each cell type; #, $p \leq 0.05$; ##, $p \leq 0.01$, significant difference between WT *versus* KO and D/A cells for the same treatment. *E*, immunoblot analyses of PKM2 (Tyr-105) and PKM2 in lysates of interscapular BAT of control (*fl/fl*) and adipose-specific PTP1B KO (*AdPTP1B-KO*) mice fed regular chow (*upper panel*) or an HFD (*lower panel*) for 30 weeks. *A.U.*, arbitrary unit.

using Coomassie Blue, and then the 60-kDa band was excised and analyzed by mass spectroscopy. This led to the identification of known PTP1B substrates, such as cortactin (35), indicating the validity of this approach. In addition, several novel putative substrates were identified, among which was pyruvate kinase.

PTP1B Regulates PKM2 Tyrosine Phosphorylation—Initially, we examined the expression of the M1 splice isoform (PKM1) of the *PKM* gene and M2 isoform (PKM2) in brown (21) and white (3T3-L1) adipose cell lines. Immunoblot analyses revealed the expression of both PKM1 and PKM2 in preadipocytes and adipocytes (differentiation days *4*, *10*, and *18*) (Fig. 1*B*). Because mass spectroscopy identified peptides that are common to PKM1 and PKM2, we investigated the coassociation of each isoform with PTP1B. PTP1B was immunoprecipitated from starved or insulin-stimulated PTP1B WT- and PTP1B D/A-reconstituted adipocytes (21), resolved using SDS-PAGE, and then immunoblotted with PKM1- and PKM2-specific antibodies (Fig. 1*C*). Significant coassociation of PTP1B D/A with PKM1 and PKM2 was observed in adipocytes upon insulin stimulation. Given the reported regulation of PKM2 by tyrosine phosphorylation (28), and because PKM2 appears to be the major isoform in adipocytes (Fig. 3), we further investigated PKM2-PTP1B interaction. We reasoned if PKM2 is a PTP1B target, then PTP1B deficiency should lead to increased PKM2 tyrosine phosphorylation. To test this, PKM2 was immunoprecipitated from starved or insulin-stimulated KO and reconstituted (WT and D/A) adipocytes and then immunoblotted with anti-phosphotyrosine antibodies. PKM2 total tyrosine phosphorylation was elevated significantly in KO and D/A compared with WT adipocytes under basal and insulin-stimulated conditions (Fig. 1*D*). PKM2 is inhibited by phosphorylation at Tyr-105 by oncogenic forms of fibroblast growth factor receptor type 1 (28). Notably, PKM2 Tyr-105 phosphorylation was elevated significantly in KO and D/A compared with WT adipocytes (Fig. 1*D*). In addition, we determined PKM2 tyrosine phosphorylation in interscapular BAT of control (fl/fl) and adipose-specific PTP1B KO (AdPTP1B-KO) mice. AdPTP1B KO mice fed chow or an HFD exhibited increased PKM2 Tyr-105 phosphorylation compared with control mice (Fig. 1*E*). Together, these data demonstrate elevated both total and Tyr^{105} phosphorylation of PKM2 upon PTP1B deficiency in adipocytes and *in vivo* suggesting that PTP1B plays an important role in regulating PKM2 activity.

Mapping of PKM2-PTP1B Interaction—Elevated PKM2 tyrosine phosphorylation upon PTP1B deficiency prompted us

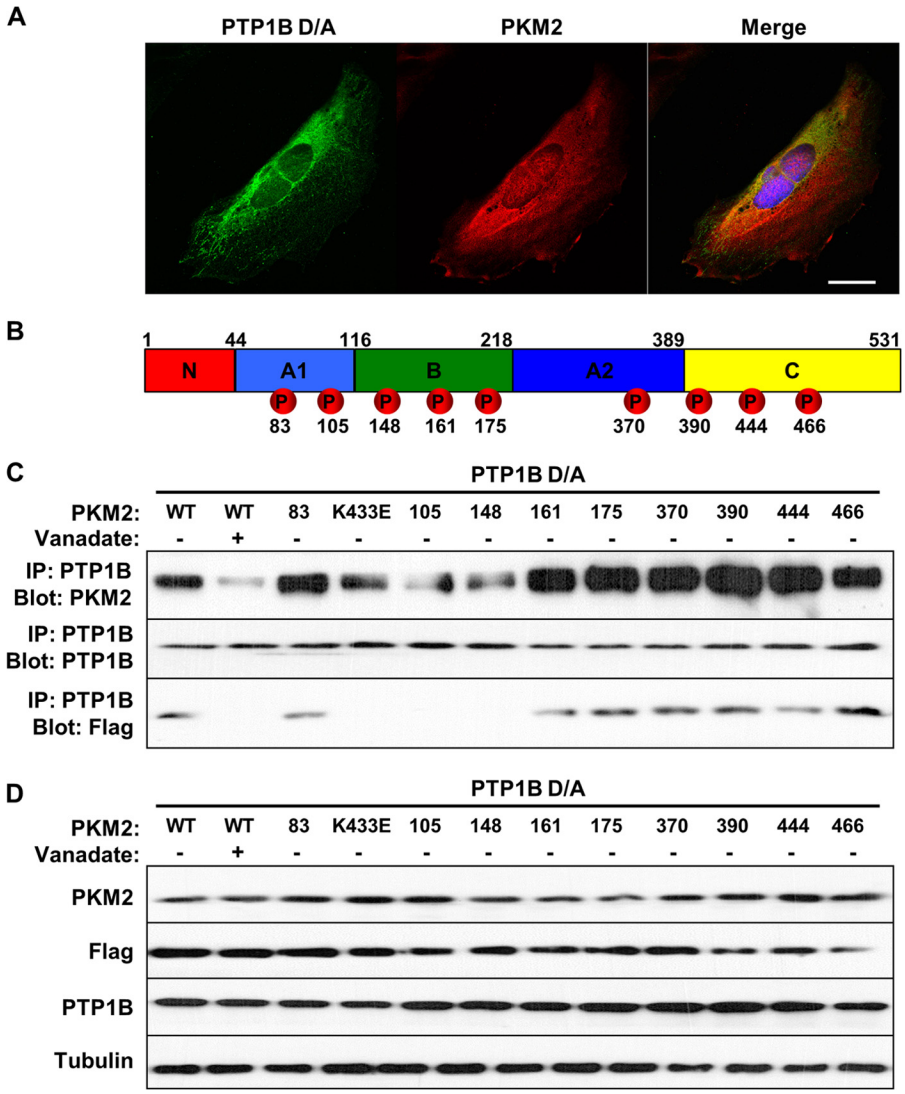

FIGURE 2. **Mapping PKM2-PTP1B sites of interaction.** *A*, immunostaining for PTP1B D/A (*green*), PKM2 (*red*), and nuclear DNA (*blue*) in preadipocytes. Cells were visualized by fluorescence confocal microscopy. *Scale bar* = 20 μm. *B*, schematic depicting PKM2 domains and tyrosine sites. *C*, PKM2 knockdown cells were reconstituted with PKM2 WT, K433E, and Y/F mutants, and cell lines were generated. PTP1B D/A was transiently expressed, immunoprecipitated (*IP*) using FG6 antibodies, resolved using SDS-PAGE, and then immunoblotted (*Blot*) for PKM2. Membranes were reprobed for PTP1B and FLAG tag (expressed by exogenous cDNA encoding PKM2 WT and mutants). *D*, immunoblots of PKM2, FLAG, PTP1B, and tubulin in total cell lysates.

to investigate whether PKM2 is a direct substrate of PTP1B. We examined the subcellular localization of PTP1B D/A and PKM2. GFP-tagged PTP1B D/A was transiently expressed in preadipocytes, and colocalization with endogenous PKM2 was monitored using confocal microscopy (Fig. 2*A*). Consistent with previous reports, PTP1B D/A localized to the endoplasmic reticulum network (11–13). Importantly, a subfraction of endogenous PKM2 colocalized with PTP1B. In addition, biochemical studies were performed to determine PTP1B-PKM2 coassociation. To that end, lentiviral shRNA was used to generate 3T3-L1 preadipocytes with stable knockdown of PKM (sh-PKM) as described under "Experimental Procedures." Knockdown cells were reconstituted with non-targetable (shRNA-resistant) cDNA encoding mouse PKM2 WT, K433E mutant, and tyrosine (Y)-to-phenylalanine (F) mutants of individual PKM2 tyrosines (Fig. 2*B*). PTP1B D/A was transiently expressed in the generated cell lines and then immunoprecipitated, and coassociation with PKM2 was determined. Consistent with the proposed hypothesis, coassociation of PKM2 WT and PTP1B D/A was observed (Fig. 2*C*, *first lane*). Treatment with pervanadate, a strong inhibitor of tyrosine phosphatases that, as a phosphate mimetic, localizes at the catalytic pocket and oxidizes the essential cysteinyl residue in the catalytic center of the enzyme (36), disrupted PKM2-PTP1B D/A association (Fig. 2*C*, *second lane*). This suggested that the association is consistent with enzyme-substrate interaction that is mediated by the active site of PTP1B. Of note, PKM2 K433E (which attenuated total tyrosine phosphorylation) (28) exhibited minimal coassociation with PTP1B D/A (Fig. 2*C*). Strikingly, mutation of single tyrosine residues Tyr-105 or Tyr-148 nearly abolished PKM2-PTP1B D/A coassociation, whereas mutations of other tyrosine residues did not significantly alter coassociation (Fig. 2, *C* and *D*). No association was observed between PKM2 and PTP1B WT, indicating that like many of its substrates, PTP1B WT does not form a stable complex with PKM2 (data not shown). Collectively, these data demonstrate that PKM2 is a

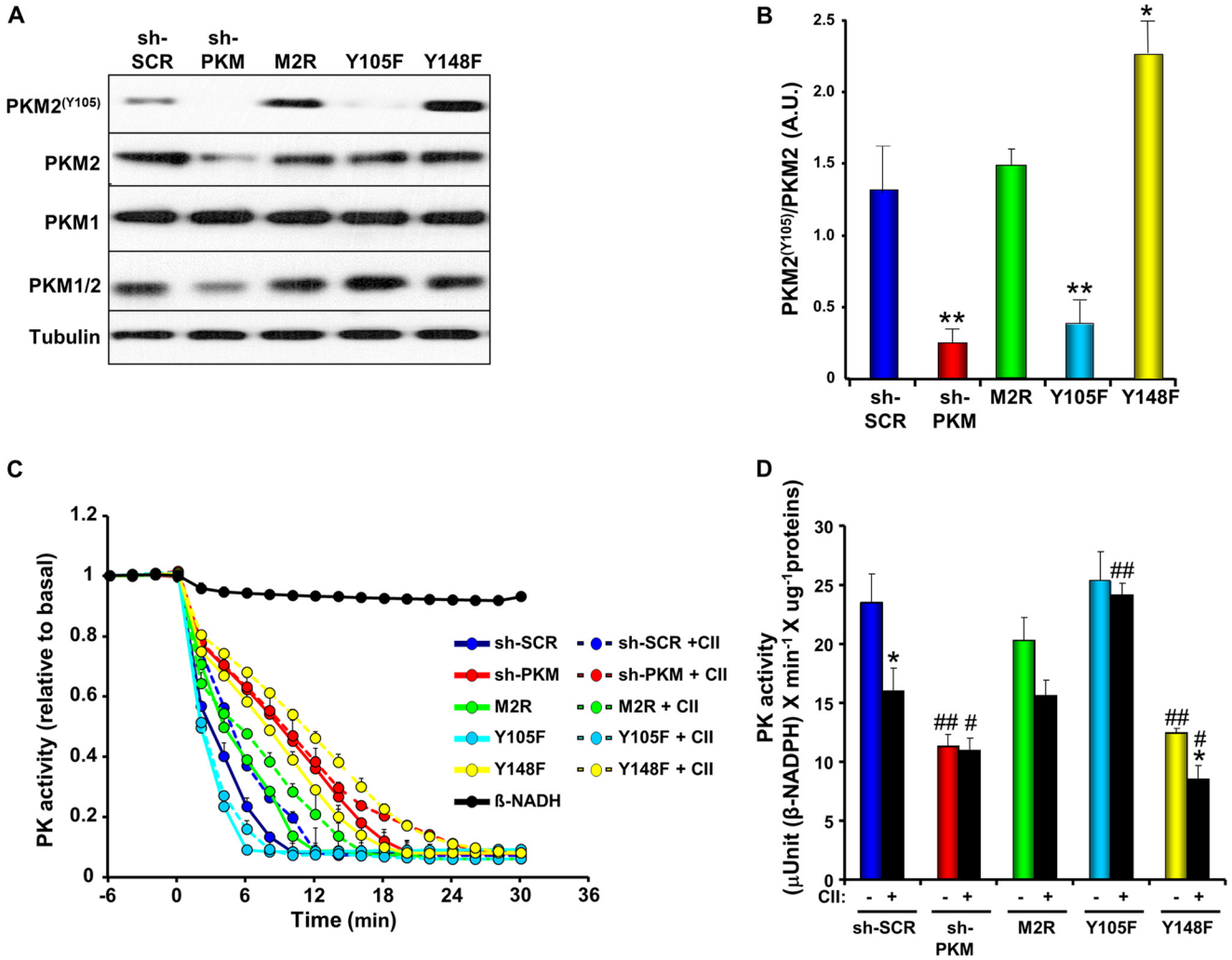

FIGURE 3. **Tyrosine phosphorylation of PKM2 regulates its activity.** Immunoblot analyses of PKM2 (Tyr-105), PKM2, PKM1, PKM1/2, and tubulin in 3T3-L1 preadipocytes expressing shRNA targeted to PKM (*sh-PKM*) or a scrambled (*SCR*) control and knockdown cells reconstituted with WT (*M2R*), Y105F, and Y148F mutants. *B*, the *bar graph* represents normalized data for PKM2 (Tyr-105)/PKM2 and presented as mean ± S.E. *, $p \leq 0.05$ and **, $p \leq 0.01$, significant difference between different cells *versus* control (*sh-SCR*). *A.U.*, arbitrary unit. *C*, total pyruvate kinase activity in sh-PKM, sh-SCR, and knockdown preadipocytes reconstituted with PKM2 WT (*M2R*) or mutants (*Y105F* and *Y148F*). Cells were treated with PTP1B inhibitor (CII), and total pyruvate kinase activity was determined (*dotted lines*). *D*, the *bar graph* represents normalized data for pyruvate kinase activity (amount of β-NADH consumed using 1 µg of protein from total cell lysates/1 min of enzymatic reaction) and presented as mean ± S.E. from two independent experiments. *, $p \leq 0.05$ and **, $p \leq 0.01$, significant difference between PTP1B inhibitor-treated *versus* non-treated for each cell type; #, $p \leq 0.05$; ##, $p \leq 0.01$, significant difference between control (*sh-SCR*) *versus* other cells for the same treatment.

direct substrate of PTP1B and that the Y105F and Y148F mutants disrupt PKM2-PTP1B D/A association significantly.

Tyrosine Phosphorylation Regulates Adipose PKM2 Activity—To investigate the role of PKM2 Tyr-105 and Tyr-148 in regulating adipose PKM2 activity, we utilized 3T3-L1 preadipocytes with stable knockdown of PKM2. Control preadipocytes were generated using a scramble shRNA (sh-SCR). To rule out off-target effects, knockdown cells were reconstituted with non-targetable cDNA encoding mouse PKM2 WT (M2R). In addition, parallel knockdown cells were reconstituted with the Y105F and Y148F mutants. Immunoblot analysis demonstrated a significant decrease in PKM2 expression in knockdown cells (Fig. 3*A*). Although the shRNA targeted a region common to PKM1 and PKM2, PKM1 protein levels did not decrease as much as PKM2 protein levels, perhaps because of PKM1 being a more stable protein. An antibody that equally recognizes PKM1 and PKM2 revealed a significant decrease in total PKM in knockdown cells (Fig. 3*A*), indicating that PKM2 accounts for the majority of pyruvate kinase in adipocytes. Consistent with this idea, total pyruvate kinase activity decreased in response to knockdown of PKM2 and was rescued by reconstitution of PKM2 (Fig. 3, *C* and *D*). Immunoblot analysis revealed significant attenuation of PKM2 Tyr-105 phosphorylation in knockdown cells (Fig. 3, *A* and *B*). As expected, Tyr-105 phosphorylation was attenuated in Y105F adipocytes, whereas Y148F adipocytes revealed increased Tyr-105 phosphorylation compared with control adipocytes. In addition, PKM2 knockdown cells exhibited a 60.8 ± 0.8% decrease in pyruvate kinase activity, whereas preadipocytes reconstituted with WT (M2R) or Y105F exhibited comparable activity to controls (Fig. 3, *C* and *D*). On the other hand, Y148F-reconstituted preadipocytes exhibited significant attenuation of pyruvate kinase activity consistent with their elevated Tyr-105 phosphorylation. Comparable pyruvate kinase activity was also observed in differen-

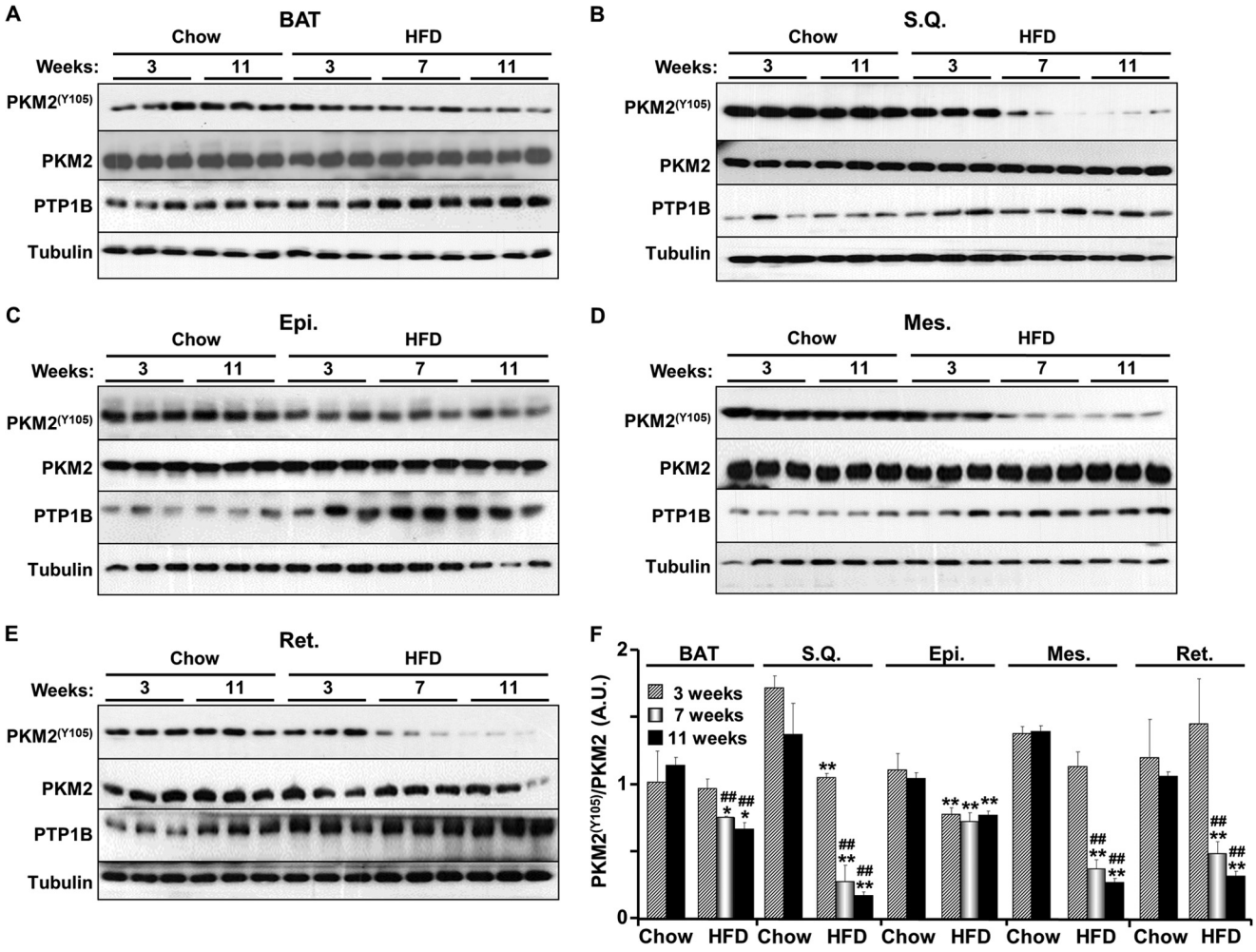

FIGURE 4. **Regulation of adipose PKM2 Tyr-105 phosphorylation by high-fat feeding.** Immunoblot analyses of PKM2 (Tyr-105), PKM2, PTP1B, and tubulin in lysates of brown (*A*), subcutaneous (*S.Q.*) (*B*), epididymal (*Epi.*) (*C*), mesenchymal (*Mes.*) (*D*), and retroperitoneal (*Ret.*) (*E*) adipose tissue depots of mice fed chow or an HFD for the indicated times. Each lane represents a sample from a separate animal. *F*, the *bar graph* represents normalized data for PKM2 (Tyr-105)/PKM2 presented as mean ± S.E. *, $p \leq 0.05$ and **, $p \leq 0.01$, significant difference between all groups *versus* mice fed a chow diet for 3 weeks; #, significant difference between mice fed an HFD for 7 and 11 weeks *versus* mice fed a HFD for 3 weeks.

tiated adipocytes (supplemental Fig. S1*A*). To further establish regulation of PKM2 phosphorylation and activity by PTP1B, preadipocytes were treated with PTP1B inhibitor (CII) as described under "Experimental Procedures." CII decreased PTP1B activity by 69.7 ± 5.4% and increased PKM2 Tyr-105 phosphorylation (supplemental Fig. S1, *B* and *C*). Notably, CII significantly decreased total pyruvate kinase activity in control (*sh-SCR*) and Y148F cells (Fig. 3, *C* and *D*). M2R cells treated with CII exhibited a trend for decreased pyruvate kinase activity but did not reach statistical significance, whereas knockdown and Y105F CII-treated cells exhibited comparable activity to non-treated cells (Fig. 3, *C* and *D*). Together, these data are consistent with previous findings that PKM2 tyrosine phosphorylation at Tyr-105 inhibits its pyruvate kinase activity.

Adipose PKM2 Tyr-105 Phosphorylation Is Regulated Nutritionally—To investigate whether adipose PKM2 phosphorylation is nutritionally regulated *in vivo,* we determined the effects of high-fat feeding on Tyr-105 phosphorylation in various adipose tissue depots. Mice were fed regular chow diet or a HFD (60% kcal from fat) starting at 7 weeks of age and then sacrificed after 3, 7, and 11 weeks. Immunoblot analyses revealed comparable PKM2 Tyr-105 phosphorylation in mice fed regular chow diet at 3 and 11 weeks in all examined adipose depots (Fig. 4). Notably, high-fat feeding for 3 weeks significantly attenuated PKM2 Tyr-105 phosphorylation in subcutaneous and epididymal depots (Fig. 4, *B*, *C*, and *F*). Prolonged high-fat feeding (7 and 11 weeks) led to significant attenuation of PKM2 Tyr-105 phosphorylation in all examined adipose depots, and this correlated with increased PTP1B expression (Fig. 4). In line with these biochemical studies, immunostaining of adipose tissue sections revealed comparable results with PKM2 Tyr-105 phosphorylation decreasing upon prolonged high-fat feeding (supplemental Fig. S2). Of note, HFD-induced attenuation of PKM2 Tyr-105 phosphorylation correlated with decreased insulin receptor (IR) (Tyr-1162/Tyr-1163) phosphorylation and decreased Akt (Ser-473) phosphorylation in adipose depots upon HFD feeding (supplemental Fig. S3). Decreased IR and Akt phosphorylation indicates decreased insulin sensitivity in HFD-fed mice compared with those fed chow. Together, these data demonstrate that adipose PKM2 Tyr-105 phosphorylation is regulated nutritionally and correlates with the development of insulin resistance in HFD-fed mice.

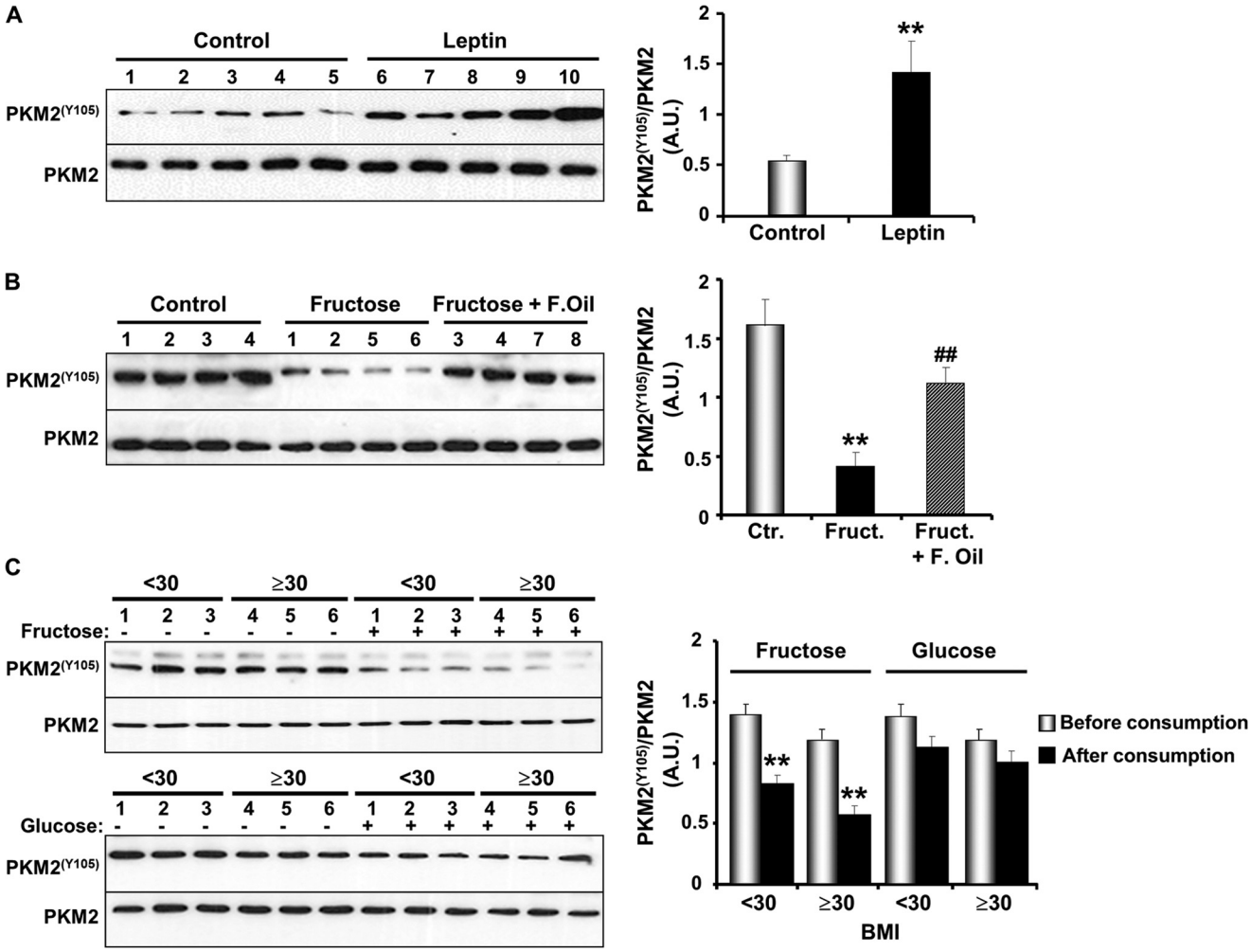

FIGURE 5. **Adipose PKM2 Tyr-105 phosphorylation correlates with systemic metabolic status.** *A*, immunoblot analyses of PKM2 (Tyr-105) and PKM2 in adipose tissue lysates from leptin-treated and non-treated (*Control*) UCD-T2DM diabetic rats. The *bar graph* represents normalized data for PKM2 (Tyr-105)/PKM2 and presented as means ± S.E. **, $p \leq 0.01$, significant difference between leptin-treated and control rats. *A.U.*, arbitrary unit. *B*, immunoblot analyses of PKM2 (Tyr-105) and PKM2 in adipose tissue lysates from rhesus monkeys that were monitored for 6 months (*Control*) and then divided into two groups: one fed fructose (*Fructose*) and the other fed fructose supplemented with fish oil (*Fructose + F. Oil*) for 6 months. The *bar graph* represents normalized data for PKM2 (Tyr-105)/PKM2, and data are presented as mean ± S.E. **, $p \leq 0.01$, significant difference between chow (*Ctr.*) *versus* fructose diets; ##, $p \leq 0.01$, significant difference between fructose (*Fruct.*) *versus* fructose with fish oil (*Fruct + F. Oil*) diets. *C*, immunoblots of PKM2 (Tyr-105) and PKM2 in lysates of subcutaneous adipose tissue biopsies from human subjects before and after consuming 25% of energy requirements as fructose-sweetened (*upper panel*) or glucose-sweetened (*lower panel*) beverage for 10 weeks. Subjects were separated into two groups: body mass index < 30 and body mass index ≥ 30. The *bar graph* represents normalized data for PKM2 (*Y105*)/PKM2 and presented as mean ± S.E. **, $p \leq 0.01$, significant difference between the same subjects before and after fructose-sweetened beverage consumption.

Adipose PKM2 Tyr-105 Phosphorylation Correlates with Systemic Metabolic Status—We investigated whether adipose PKM2 Tyr-105 phosphorylation directly correlates with an altered metabolic state (independently of HFD-induced obesity) and whether this is conserved among species. To that end, we utilized different experimental models including rats, non-human primates, and human subjects who were subjected to different interventions that altered their metabolic state. Firstly, we used UCD-T2DM diabetic rats, which exhibit adult onset polygenic obesity and insulin resistance and subsequently develop type 2 diabetes (37). Leptin administration to diabetic UCD-T2DM rats normalizes fasting plasma glucose concentrations and markedly improves insulin sensitivity independently of food intake (38). Diabetic UCD-T2DM rats received leptin (murine recombinant, 0.5 mg/kg) or saline injections (control). Importantly, saline-injected animals were pair-fed to the leptin-treated animals to control for food intake, and tissues were collected after one month of treatment. Immunoblot analyses revealed increased PKM2 Tyr-105 phosphorylation in white adipose tissue of the leptin-treated rats compared with controls (Fig. 5*A*). Consistent with the improved insulin sensitivity in leptin-treated rats (38), they exhibited increased IR and Akt phosphorylation compared with controls (supplemental Fig. S4*A*). Thus, adipose PKM2 Tyr-105 phosphorylation increases upon improved systemic insulin sensitivity independently of significant alterations in body weight.

Next, we investigated the regulation of PKM2 Tyr-105 phosphorylation in a non-human primate model of insulin resistance, fructose-fed rhesus macaques (39). Base-line adipose samples were collected (*Control*), and animals were divided into two groups: one fed fructose (*Fructose*) and another fed fructose supplemented with fish oil (*Fructose + F. Oil*) for 6

months as detailed under "Experimental Procedures." Animals fed fructose progressively developed glucose intolerance and decreased insulin sensitivity (39). Immunoblot analyses of subcutaneous adipose tissue revealed that PKM2 Tyr-105 phosphorylation was decreased significantly in the fructose-fed group compared with controls (Fig. 5*B*). On the other hand, the animals supplemented with fish oil exhibited PKM2 Tyr-105 phosphorylation that was comparable with controls. In addition, PKM2 Tyr-105 phosphorylation correlated with IR and Akt phosphorylation, which decreased in the fructose-fed group compared with controls and increased with fish oil supplementation (supplemental Fig. S4*B*).

Lastly, to determine whether findings from these animal models translate to humans, we analyzed PKM2 Tyr-105 phosphorylation in human subcutaneous adipose tissues from subjects that developed insulin resistance while consuming fructose-sweetened beverages. Subjects were provided 25% of energy requirements from glucose- or fructose-sweetened beverages for 10 weeks. Subjects consuming fructose, but not those consuming glucose beverages, exhibited increased fasting plasma glucose and decreased insulin sensitivity (40). Immunoblot analyses of subcutaneous adipose tissue in fructose-fed overweight (body mass index < 30) or obese (body mass index ≥ 30) subjects exhibited decreased PKM2 Tyr-105 phosphorylation after fructose feeding (Fig. 5*C*). In contrast, Tyr-105 phosphorylation did not change significantly in subcutaneous adipose tissue samples from subjects consuming glucose-sweetened beverages (Fig. 5*C*). Collectively, these results demonstrate that adipose PKM2 Tyr-105 phosphorylation directly correlates with the metabolic state in different species. Whether alterations in Tyr-105 phosphorylation are causative or consequences of the metabolic state remain to be determined.

DISCUSSION

The coordinated actions of protein tyrosine phosphatases and protein tyrosine kinases regulate phosphotyrosine-mediated signaling under physiological and pathophysiological conditions. Understanding the dynamic modulation of phosphotyrosine signaling in adipose tissue may provide avenues for therapeutic intervention in metabolic diseases. In this study, we identified PKM2 as a novel PTP1B substrate in adipocytes and adipose depots *in vivo* and determined PKM2 Tyr-105 and Tyr148 as key residues that mediated the interaction. In addition, we demonstrated regulation of PKM2 pyruvate kinase activity in adipocytes by tyrosine phosphorylation. Further, we uncovered direct correlation of adipose PKM2 Tyr-105 phosphorylation with the systemic metabolic state in rodents, nonhuman primates, and humans. Collectively, these findings provide new insights into the regulation of adipose PKM2 by tyrosine phosphorylation and its metabolic function.

Several lines of evidence established PKM2 as a novel PTP1B substrate. First, mass spectrometry of adipocytes expressing the PTP1B-trapping mutant identified PKM as a PTP1B-interacting protein. Second, adipocytes and adipose tissue lacking PTP1B exhibited increased PKM2 total and Tyr-105 phosphorylation. Third, substrate trapping demonstrated a direct association between PKM2 and PTP1B D/A. Importantly, pervanadate treatment disrupted PKM2-PTP1B D/A association, indicating that it is consistent with enzyme-substrate interaction that is mediated by the PTP1B active site. Fourth, pharmacological inhibition of PTP1B with a PTP1B-specific small molecule inhibitor (CII) increased PKM2 Tyr-105 phosphorylation and attenuated pyruvate kinase activity. At the molecular level, we identified PKM2 Tyr-105 and Tyr-148 as key residues that mediate interaction with PTP1B. However, the residue that serves as the primary interaction site remains to be delineated. The observed disruption of PTP1B D/A-PKM2 Y148F interaction (Fig. 2), despite increased Tyr-105 phosphorylation in Y148F-expressing adipocytes (Fig. 3), indicates that Tyr-148 is important for binding of PKM2 to PTP1B. Of note, PKM2 Y105F mutation also disrupts PTP1B D/A-PKM2 interaction (Fig. 2). In addition to adipose tissue, PKM2 is expressed in other differentiated tissues such as lung, retina, pancreatic islets, and proliferating cells (such as embryonic cells, adult stem cells, and especially tumor cells) (25, 41). Further studies are required to determine whether PKM2 and PTP1B interact in other tissue(s). Indeed, both PTP1B (42) and PKM2 are expressed in pancreatic islets, and preliminary studies suggest coassociation in pancreatic lysates[5]. PTP1B-catalyzed dephosphorylation of its substrates is regulated, at least in part, by its subcellular location on the cytoplasmic face of the endoplasmic reticulum, which imposes topological constraints (11, 43). Thus, endoplasmic reticulum-bound PTP1B can access and dephosphorylate cytosolic PKM2 but presumably not other pools, such as nuclear PKM2. Several studies report PKM2 nuclear translocation and demonstrate a role in activating gene transcription and cell proliferation (44–47). It is possible that other protein tyrosine phosphatase(s) may also target PKM2 at various subcellular locations, including the nucleus. Overall, although additional studies are needed to dissect the spatial and temporal regulation of PKM2-PTP1B interaction and uncover other candidate PTPs, these studies are the first to identify a protein tyrosine phosphatase that directly regulates PKM2 tyrosine phosphorylation and activity.

PKM2 tyrosine phosphorylation regulates its pyruvate kinase activity in adipocytes. Using an *in vitro* adipocyte cell system we demonstrated a direct effect of Tyr-105 phosphorylation on PKM2 activity (Fig. 3). Indeed, PKM2 Y148F adipocytes exhibited increased Tyr-105 phosphorylation and significant attenuation of PKM2 pyruvate kinase activity. This is consistent with previous findings that PKM2 tyrosine phosphorylation at Tyr-105 inhibits its pyruvate kinase activity (28). Notably, PTP1B deficiency or inhibition in adipocytes increased PKM2 Tyr-105 phosphorylation. The precise contribution of adipose PKM2 tyrosine phosphorylation to metabolic regulation remains to be determined. However, this study clearly demonstrated attenuation of PKM2 Tyr-105 phosphorylation in BAT and white adipose tissue depots with prolonged high-fat feeding in mice concomitant with increased PTP1B expression in these depots (Fig. 4). Importantly, elevated PKM2 Tyr-105 phosphorylation correlated with increased insulin sensitivity and decreased Tyr-105 phosphorylation correlated with insulin resistance in rodents,

[5] A. Bettaieb and F. G. Haj, unpublished data.

non-human primates, and humans. Additional studies are warranted to delineate the role of adipose PKM2 in metabolic regulation and to determine whether alterations in PKM2 Tyr-105 phosphorylation are causative or a consequence of the metabolic state *in vivo*.

The metabolic functions of adipose PTP1B are unresolved, with studies demonstrating detrimental, beneficial, or no effects of adipose PTP1B deficiency on body mass regulation and insulin sensitivity. Antisense oligonucleotides that lower PTP1B levels only in adipose tissue and liver reduce diet-induced obesity and enhance insulin signaling in obese (*ob/ob*) and diabetic (*db/db*) mice (48, 49). Similarly, administration of PTP1B antisense oligonucleotides to monkeys reduces PTP1B in adipose tissue and liver and improves insulin sensitivity (50). The observed effects could reflect a loss of PTP1B in liver and/or adipose tissue. On the other hand, adipose-specific PTP1B KO mice generated using the adipocyte protein 2 (aP2)-promoter to drive Cre recombinase expression exhibit increased body weight when fed an HFD (19). However, if the observed weight gain is caused only by adipose-specific PTP1B deficiency remains to be determined because the aP2 promoter can delete the target gene in other cell types (51, 52). Indeed, adipose-specific PTP1B KO mice generated using the adiponectin promoter exhibit comparable body weight to controls when fed an HFD but display larger adipocytes and increased basal lipogenesis (20). These studies identify PKM2 as one of several PTP1B substrates that can mediate PTP1B functions in adipose tissue. Presumably PTP1B can engage different substrate(s) in adipocytes, depending, at least in part, on the nature of the challenge/stimulus and its magnitude and duration. Intriguingly, adipose PTP1B function could vary, depending on the adipose depot. PTP1B inhibition in 3T3-L1 adipocytes inhibits adipogenesis (53). In contrast, PTP1B deficiency in brown adipocytes promotes differentiation and adipogenesis (21, 54).

The salutary effects of PTP1B deficiency and inhibition make it a therapeutic target for obesity, type 2 diabetes, and some types of cancer (55, 56). In addition, PKM2 plays important roles in cancer cells signaling and metabolism and is proposed as an attractive therapeutic target. PKM2 deficiency or inhibition elicits anticancer effects, such as impairment of cancer growth, induction of cell death, and increased sensitivity to chemotherapy (27, 57–59). On the other hand, compounds that activate PKM2 catalytic function may also have therapeutic implications to suppress tumorigenesis (60–62). The regulation of PKM2 activity in adipose tissue by tyrosine phosphorylation as presented here highlights the need to evaluate PKM2 functions in normal tissues before inhibitors and activators are deployed for therapeutic interventions. Dissecting the intracellular signaling events elicited by PTP1B and PKM2 will likely yield valuable insights and may lead to new avenues for therapeutic intervention.

Acknowledgments—We thank Dr. Benjamin Neel (Ontario Cancer Institute) for PTP1B floxed mice and Dr. Evan Rosen (BIDMC/Harvard University) for Adiponectin-Cre mice.

REFERENCES

1. Mann, J. I. (2002) Diet and risk of coronary heart disease and type 2 diabetes. *Lancet* **360,** 783–789
2. Rosen, E. D., and Spiegelman, B. M. (2006) Adipocytes as regulators of energy balance and glucose homeostasis. *Nature* **444,** 847–853
3. Farmer, S. R. (2008) Molecular determinants of brown adipocyte formation and function. *Genes Dev.* **22,** 1269–1275
4. Enerbäck, S. (2010) Human brown adipose tissue. *Cell Metab.* **11,** 248–252
5. Nandi, A., Kitamura, Y., Kahn, C. R., and Accili, D. (2004) Mouse models of insulin resistance. *Physiol. Rev.* **84,** 623–647
6. Taniguchi, C. M., Emanuelli, B., and Kahn, C. R. (2006) Critical nodes in signalling pathways. Insights into insulin action. *Nat. Rev. Mol. Cell Biol.* **7,** 85–96
7. Zhang, Y., Proenca, R., Maffei, M., Barone, M., Leopold, L., and Friedman, J. M. (1994) Positional cloning of the mouse obese gene and its human homologue. *Nature* **372,** 425–432
8. Friedman, J. M., and Halaas, J. L. (1998) Leptin and the regulation of body weight in mammals. *Nature* **395,** 763–770
9. Flier, J. S. (2004) Obesity wars: molecular progress confronts an expanding epidemic. *Cell* **116,** 337–350
10. Tonks, N. K. (2006) Protein tyrosine phosphatases. From genes, to function, to disease. *Nat. Rev. Mol. Cell Biol.* **7,** 833–846
11. Frangioni, J. V., Beahm, P. H., Shifrin, V., Jost, C. A., and Neel, B. G. (1992) The nontransmembrane tyrosine phosphatase PTP-1B localizes to the endoplasmic reticulum via its 35 amino acid C-terminal sequence. *Cell* **68,** 545–560
12. Woodford-Thomas, T. A., Rhodes, J. D., and Dixon, J. E. (1992) Expression of a protein tyrosine phosphatase in normal and v-src-transformed mouse 3T3 fibroblasts. *J. Cell Biol.* **117,** 401–414
13. Haj, F. G., Verveer, P. J., Squire, A., Neel, B. G., and Bastiaens, P. I. (2002) Imaging sites of receptor dephosphorylation by PTP1B on the surface of the endoplasmic reticulum. *Science* **295,** 1708–1711
14. Elchebly, M., Payette, P., Michaliszyn, E., Cromlish, W., Collins, S., Loy, A. L., Normandin, D., Cheng, A., Himms-Hagen, J., Chan, C. C., Ramachandran, C., Gresser, M. J., Tremblay, M. L., and Kennedy, B. P. (1999) Increased insulin sensitivity and obesity resistance in mice lacking the protein tyrosine phosphatase-1B gene. *Science* **283,** 1544–1548
15. Klaman, L. D., Boss, O., Peroni, O. D., Kim, J. K., Martino, J. L., Zabolotny, J. M., Moghal, N., Lubkin, M., Kim, Y. B., Sharpe, A. H., Stricker-Krongrad, A., Shulman, G. I., Neel, B. G., and Kahn, B. B. (2000) Increased energy expenditure, decreased adiposity, and tissue-specific insulin sensitivity in protein-tyrosine phosphatase 1B-deficient mice. *Mol. Cell. Biol.* **20,** 5479–5489
16. Delibegovic, M., Bence, K. K., Mody, N., Hong, E. G., Ko, H. J., Kim, J. K., Kahn, B. B., and Neel, B. G. (2007) Improved glucose homeostasis in mice with muscle-specific deletion of protein-tyrosine phosphatase 1B. *Mol. Cell. Biol.* **27,** 7727–7734
17. Haj, F. G., Zabolotny, J. M., Kim, Y. B., Kahn, B. B., and Neel, B. G. (2005) Liver-specific protein-tyrosine phosphatase 1B (PTP1B) re-expression alters glucose homeostasis of PTP1B$^{-/-}$ mice. *J. Biol. Chem.* **280,** 15038–15046
18. Delibegovic, M., Zimmer, D., Kauffman, C., Rak, K., Hong, E. G., Cho, Y. R., Kim, J. K., Kahn, B. B., Neel, B. G., and Bence, K. K. (2009) Liver-specific deletion of protein-tyrosine phosphatase 1B (PTP1B) improves metabolic syndrome and attenuates diet-induced endoplasmic reticulum stress. *Diabetes* **58,** 590–599
19. Bence, K. K., Delibegovic, M., Xue, B., Gorgun, C. Z., Hotamisligil, G. S., Neel, B. G., and Kahn, B. B. (2006) Neuronal PTP1B regulates body weight, adiposity and leptin action. *Nat. Med.* **12,** 917–924
20. Owen, C., Czopek, A., Agouni, A., Grant, L., Judson, R., Lees, E. K., Mcilroy, G. D., Göransson, O., Welch, A., Bence, K. K., Kahn, B. B., Neel, B. G., Mody, N., and Delibegovi, M. (2012) Adipocyte-specific protein tyrosine phosphatase 1B deletion increases lipogenesis, adipocyte cell size and is a minor regulator of glucose homeostasis. *PloS ONE* **7,** e32700
21. Matsuo, K., Bettaieb, A., Nagata, N., Matsuo, I., Keilhack, H., and Haj, F. G. (2011) Regulation of brown fat adipogenesis by protein tyrosine phospha-

tase 1B. *PloS ONE* **6,** e16446
22. Bettaieb, A., Matsuo, K., Matsuo, I., Wang, S., Melhem, R., Koromilas, A. E., and Haj, F. G. (2012) Protein tyrosine phosphatase 1B deficiency potentiates PERK/eIF2α signaling in brown adipocytes. *PloS ONE* **7,** e34412
23. Krishnan, N., Fu, C., Pappin, D. J., and Tonks, N. K. (2011) H2S-Induced sulfhydration of the phosphatase PTP1B and its role in the endoplasmic reticulum stress response. *Sci. Signal.* **4,** ra86
24. Kayne, F. J., and Price, N. C. (1973) Amino acid effector binding to rabbit muscle pyruvate kinase. *Arch. Biochem. Biophys.* **159,** 292–296
25. Jurica, M. S., Mesecar, A., Heath, P. J., Shi, W., Nowak, T., and Stoddard, B. L. (1998) The allosteric regulation of pyruvate kinase by fructose-1,6-bisphosphate. *Structure* **6,** 195–210
26. Christofk, H. R., Vander Heiden, M. G., Wu, N., Asara, J. M., and Cantley, L. C. (2008) Pyruvate kinase M2 is a phosphotyrosine-binding protein. *Nature* **452,** 181–186
27. Christofk, H. R., Vander Heiden, M. G., Harris, M. H., Ramanathan, A., Gerszten, R. E., Wei, R., Fleming, M. D., Schreiber, S. L., and Cantley, L. C. (2008) The M2 splice isoform of pyruvate kinase is important for cancer metabolism and tumour growth. *Nature* **452,** 230–233
28. Hitosugi, T., Kang, S., Vander Heiden, M. G., Chung, T. W., Elf, S., Lythgoe, K., Dong, S., Lonial, S., Wang, X., Chen, G. Z., Xie, J., Gu, T. L., Polakiewicz, R. D., Roesel, J. L., Boggon, T. J., Khuri, F. R., Gilliland, D. G., Cantley, L. C., Kaufman, J., and Chen, J. (2009) Tyrosine phosphorylation inhibits PKM2 to promote the Warburg effect and tumor growth. *Sci. Signal* **2,** ra73
29. Xie, L., Lee, S. Y., Andersen, J. N., Waters, S., Shen, K., Guo, X. L., Moller, N. P., Olefsky, J. M., Lawrence, D. S., and Zhang, Z. Y. (2003) Cellular effects of small molecule PTP1B inhibitors on insulin signaling. *Biochemistry* **42,** 12792–12804
30. Anastasiou, D., Poulogiannis, G., Asara, J. M., Boxer, M. B., Jiang, J. K., Shen, M., Bellinger, G., Sasaki, A. T., Locasale, J. W., Auld, D. S., Thomas, C. J., Vander Heiden, M. G., and Cantley, L. C. (2011) Inhibition of pyruvate kinase M2 by reactive oxygen species contributes to cellular antioxidant responses. *Science* **334,** 1278–1283
31. Breitkopf, S. B., and Asara, J. M. (2012) Determining *in vivo* phosphorylation sites using mass spectrometry in *Current Protocols in Molecular Biology* (Ausubel, F. M., eds) pp. 1–27, Edison, New Jersey
32. Zhang, Z. Y., Maclean, D., McNamara, D. J., Sawyer, T. K., and Dixon, J. E. (1994) Protein tyrosine phosphatase substrate specificity. Size and phosphotyrosine positioning requirements in peptide substrates. *Biochemistry* **33,** 2285–2290
33. Flint, A. J., Tiganis, T., Barford, D., and Tonks, N. K. (1997) Development of "substrate-trapping" mutants to identify physiological substrates of protein tyrosine phosphatases. *Proc. Natl. Acad. Sci. U.S.A.* **94,** 1680–1685
34. Haj, F. G., Markova, B., Klaman, L. D., Bohmer, F. D., and Neel, B. G. (2003) Regulation of receptor tyrosine kinase signaling by protein tyrosine phosphatase-1B. *J. Biol. Chem.* **278,** 739–744
35. Stuible, M., Dubé, N., and Tremblay, M. L. (2008) PTP1B regulates cortactin tyrosine phosphorylation by targeting Tyr-446. *J. Biol. Chem.* **283,** 15740–15746
36. Huyer, G., Liu, S., Kelly, J., Moffat, J., Payette, P., Kennedy, B., Tsaprailis, G., Gresser, M. J., and Ramachandran, C. (1997) Mechanism of inhibition of protein-tyrosine phosphatases by vanadate and pervanadate. *J. Biol. Chem.* **272,** 843–851
37. Cummings, B. P., Digitale, E. K., Stanhope, K. L., Graham, J. L., Baskin, D. G., Reed, B. J., Sweet, I. R., Griffen, S. C., and Havel, P. J. (2008) Development and characterization of a novel rat model of type 2 diabetes mellitus. The UC Davis type 2 diabetes mellitus UCD-T2DM rat. *Am. J. Physiol. Regul. Integr. Comp. Physiol.* **295,** R1782–1793
38. Cummings, B. P., Bettaieb, A., Graham, J. L., Stanhope, K. L., Dill, R., Morton, G. J., Haj, F. G., and Havel, P. J. (2011) Subcutaneous administration of leptin normalizes fasting plasma glucose in obese type 2 diabetic UCD-T2DM rats. *Proc. Natl. Acad. Sci. U.S.A.* **108,** 14670–14675
39. Bremer, A. A., Stanhope, K. L., Graham, J. L., Cummings, B. P., Wang, W., Saville, B. R., and Havel, P. J. (2011) Fructose-fed rhesus monkeys: a nonhuman primate model of insulin resistance, metabolic syndrome, and type 2 diabetes. *Clin. Transl. Sci.* **4,** 243–252
40. Stanhope, K. L., Schwarz, J. M., Keim, N. L., Griffen, S. C., Bremer, A. A., Graham, J. L., Hatcher, B., Cox, C. L., Dyachenko, A., Zhang, W., McGahan, J. P., Seibert, A., Krauss, R. M., Chiu, S., Schaefer, E. J., Ai, M., Otokozawa, S., Nakajima, K., Nakano, T., Beysen, C., Hellerstein, M. K., Berglund, L., and Havel, P. J. (2009) Consuming fructose-sweetened, not glucose-sweetened, beverages increases visceral adiposity and lipids and decreases insulin sensitivity in overweight/obese humans. *J. Clin. Invest.* **119,** 1322–1334
41. Yamada, K., and Noguchi, T. (1999) Regulation of pyruvate kinase M gene expression. *Biochem. Biophys. Res. Commun.* **256,** 257–262
42. Bettaieb, A., Liu, S., Xi, Y., Nagata, N., Matsuo, K., Matsuo, I., Chahed, S., Bakke, J., Keilhack, H., Tiganis, T., and Haj, F. G. (2011) Differential regulation of endoplasmic reticulum stress by protein tyrosine phosphatase 1B and T cell protein tyrosine phosphatase. *J. Biol. Chem.* **286,** 9225–9235
43. Haj, F. G., Sabet, O., Kinkhabwala, A., Wimmer-Kleikamp, S., Roukos, V., Han, H. M., Grabenbauer, M., Bierbaum, M., Antony, C., Neel, B. G., and Bastiaens, P. I. (2012). Regulation of signaling at regions of cell-cell contact by endoplasmic reticulum-bound protein-tyrosine phosphatase 1B. *PloS ONE* **7,** e36633
44. Lee, J., Kim, H. K., Han, Y. M., and Kim, J. (2008) Pyruvate kinase isozyme type M2 (PKM2) interacts and cooperates with Oct-4 in regulating transcription. *Int. J. Biochem. Cell Biol.* **40,** 1043–1054
45. Hoshino, A., Hirst, J. A., and Fujii, H. (2007) Regulation of cell proliferation by interleukin-3-induced nuclear translocation of pyruvate kinase. *J. Biol. Chem.* **282,** 17706–17711
46. Luo, W., Hu, H., Chang, R., Zhong, J., Knabel, M., O'Meally, R., Cole, R. N., Pandey, A., and Semenza, G. L. (2011) Pyruvate kinase M2 is a PHD3-stimulated coactivator for hypoxia-inducible factor 1. *Cell* **145,** 732–744
47. Yang, W., Xia, Y., Ji, H., Zheng, Y., Liang, J., Huang, W., Gao, X., Aldape, K., and Lu, Z. (2011) Nuclear PKM2 regulates β-catenin transactivation upon EGFR activation. *Nature* **480,** 118–122
48. Rondinone, C. M., Trevillyan, J. M., Clampit, J., Gum, R. J., Berg, C., Kroeger, P., Frost, L., Zinker, B. A., Reilly, R., Ulrich, R., Butler, M., Monia, B. P., Jirousek, M. R., and Waring, J. F. (2002) Protein tyrosine phosphatase 1B reduction regulates adiposity and expression of genes involved in lipogenesis. *Diabetes* **51,** 2405–2411
49. Zinker, B. A., Rondinone, C. M., Trevillyan, J. M., Gum, R. J., Clampit, J. E., Waring, J. F., Xie, N., Wilcox, D., Jacobson, P., Frost, L., Kroeger, P. E., Reilly, R. M., Koterski, S., Opgenorth, T. J., Ulrich, R. G., Crosby, S., Butler, M., Murray, S. F., McKay, R. A., Bhanot, S., Monia, B. P., and Jirousek, M. R. (2002) PTP1B antisense oligonucleotide lowers PTP1B protein, normalizes blood glucose, and improves insulin sensitivity in diabetic mice. *Proc. Natl. Acad. Sci. U.S.A.* **99,** 11357–11362
50. Swarbrick, M. M., Havel, P. J., Levin, A. A., Bremer, A. A., Stanhope, K. L., Butler, M., Booten, S. L., Graham, J. L., McKay, R. A., Murray, S. F., Watts, L. M., Monia, B. P., and Bhanot, S. (2009) Inhibition of protein tyrosine phosphatase-1B with antisense oligonucleotides improves insulin sensitivity and increases adiponectin concentrations in monkeys. *Endocrinology* **150,** 1670–1679
51. Makowski, L., Boord, J. B., Maeda, K., Babaev, V. R., Uysal, K. T., Morgan, M. A., Parker, R. A., Suttles, J., Fazio, S., Hotamisligil, G. S., and Linton, M. F. (2001) Lack of macrophage fatty-acid-binding protein aP2 protects mice deficient in apolipoprotein E against atherosclerosis. *Nat. Med.* **7,** 699–705
52. Urs, S., Harrington, A., Liaw, L., and Small, D. (2006) Selective expression of an aP2/fatty acid binding protein 4-Cre transgene in non-adipogenic tissues during embryonic development. *Transgenic Res.* **15,** 647–653
53. Muthusamy, V. S., Anand, S., Sangeetha, K. N., Sujatha, S., Arun, B., and Lakshmi, B. S. (2008) Tannins present in *Cichorium intybus* enhance glucose uptake and inhibit adipogenesis in 3T3-L1 adipocytes through PTP1B inhibition. *Chem. Biol. Interact.* **174,** 69–78
54. Miranda, S., González-Rodríguez, A., Revuelta-Cervantes, J., Rondinone, C. M., and Valverde, A. M. (2010) Beneficial effects of PTP1B deficiency on brown adipocyte differentiation and protection against apoptosis induced by pro- and anti-inflammatory stimuli. *Cell. Signal.* **22,** 645–659
55. Johnson, T. O., Ermolieff, J., and Jirousek, M. R. (2002) Protein tyrosine phosphatase 1B inhibitors for diabetes. *Nat. Rev. Drug Discov.* **1,** 696–709
56. Ramachandran, C., and Kennedy, B. P. (2003) Protein tyrosine phospha-

tase 1B. A novel target for type 2 diabetes and obesity. *Curr. Top. Med. Chem.* **3,** 749–757
57. Goldberg, M. S., and Sharp, P. A. (2012) Pyruvate kinase M2-specific siRNA induces apoptosis and tumor regression. *J. Exp. Med.* **209,** 217–224
58. Spoden, G. A., Mazurek, S., Morandell, D., Bacher, N., Ausserlechner, M. J., Jansen-Dürr, P., Eigenbrodt, E., and Zwerschke, W. (2008) Isotype-specific inhibitors of the glycolytic key regulator pyruvate kinase subtype M2 moderately decelerate tumor cell proliferation. *Int. J. Cancer* **123,** 312–321
59. Macintyre, A. N., and Rathmell, J. C. (2011) PKM2 and the tricky balance of growth and energy in cancer. *Mol. Cell* **42,** 713–714
60. Jiang, J. K., Boxer, M. B., Vander Heiden, M. G., Shen, M., Skoumbourdis, A. P., Southall, N., Veith, H., Leister, W., Austin, C. P., Park, H. W., Inglese, J., Cantley, L. C., Auld, D. S., and Thomas, C. J. (2010) Evaluation of thieno[3,2-b]pyrrole[3,2-d]pyridazinones as activators of the tumor cell specific M2 isoform of pyruvate kinase. *Bioorg. Med. Chem. Lett.* **20,** 3387–3393
61. Boxer, M. B., Jiang, J. K., Vander Heiden, M. G., Shen, M., Skoumbourdis, A. P., Southall, N., Veith, H., Leister, W., Austin, C. P., Park, H. W., Inglese, J., Cantley, L. C., Auld, D. S., and Thomas, C. J. (2010) Evaluation of substituted N,N′-diarylsulfonamides as activators of the tumor cell specific M2 isoform of pyruvate kinase. *J. Med. Chem.* **53,** 1048–1055
62. Anastasiou, D., Yu, Y., Israelsen, W. J., Jiang, J. K., Boxer, M. B., Hong, B. S., Tempel, W., Dimov, S., Shen, M., Jha, A., Yang, H., Mattaini, K. R., Metallo, C. M., Fiske, B. P., Courtney, K. D., Malstrom, S., Khan, T. M., Kung, C., Skoumbourdis, A. P., Veith, H., Southall, N., Walsh, M. J., Brimacombe, K. R., Leister, W., Lunt, S. Y., Johnson, Z. R., Yen, K. E., Kunii, K., Davidson, S. M., Christofk, H. R., Austin, C. P., Inglese, J., Harris, M. H., Asara, J. M., Stephanopoulos, G., Salituro, F. G., Jin, S., Dang, L., Auld, D. S., Park, H. W., Cantley, L. C., Thomas, C. J., and Vander Heiden, M. G. (2012) Pyruvate kinase M2 activators promote tetramer formation and suppress tumorigenesis. *Nat. Chem. Biol.* **8,** 839–847

SUPPLEMENTARY FIGURE LEGENDS

Figure S1: Regulation of pyruvate kinase activity by tyrosine phosphorylation. Total pyruvate kinase activity in differentiated 3T3-L1 adipocytes expressing shRNA targeted to PKM (sh-PKM) or a scrambled (SCR) control and knockdown cells reconstituted with WT (M2R), Y105F and Y148F mutants. Bar graph represents normalized data for pyruvate kinase activity and presented as means ± SEM from two independent experiments. (*) indicates significant difference between control (sh-SCR) versus other cells. **B**) 3T3-Ll preadipocytes treated were with PTP1B inhibitor (CII; 200 nM) for 12 h and PTP1B activity was determined. (*) indicates significant difference between treated and untreated cells. **C**) Immunoblots of PKM2 (Tyr105), PKM2 and Tubulin in lysates of sh-PKM and sh-SCR preadipocytes without (-) or with (+) PTP1B inhibitor treatment.

Figure S2: Immunostaining of PKM2 and Tyr^{105} in adipose depots. Brown (BAT), epididymal (Epi.) and mesenchymal (Mes.) adipose sections of wild type male mice fed regular chow or HFD for 3 and 11 weeks were immunostained using PKM2 and Tyr105 antibodies.

Figure S3: Decreased IR and Akt phosphorylation in adipose depots of mice fed HFD. Immunoblots of pIR (Y1162/Y1163), IR, pAkt (S473), and Akt in lysates of (**A**) brown (BAT), (**B**) subcutaneous (S.Q.), (**C**) epididymal (Epi.), (**D**) mesenchymal (Mes.), and (**E**) retroperitoneal (Ret.) adipose tissue depots of mice fed chow or HFD for the indicated times. Each lane represents a sample from a separate animal. Bar graphs represent normalized data for pIR (Y1162/Y1163)/IR (**F**) and pAkt (S473)/Akt (**G**) presented as means ± SEM. (*) indicates significant difference between all groups versus mice fed chow diet for 3 weeks, (#) indicates significant difference between mice fed HFD for 7 and 11 weeks versus mice fed HFD for 3 weeks.

Figure S4: IR and Akt phosphorylation in adipose tissue of rats and rhesus monkeys. A) Immunoblots of pIR (Y1162/Y1163), IR, pAkt (S473) and Akt in lysates of adipose tissues from leptin treated and non-treated UCD-T2DM diabetic rats. Bar graphs represent normalized data for pIR (Y1162/Y1163)/IR and pAkt (S473)/Akt, and presented as means ± SEM. (*) indicates significant difference between leptin treated and control rats. **B**) Immunoblots of pIR (Y1162/Y1163), IR, pAkt (S473) and Akt in lysates of adipose tissues from rhesus monkeys that were divided into two study groups; one fed fructose (Fructose) and the other fed fructose supplemented with fish oil (Fructose + F. Oil) for 6 months. Bar graphs represent normalized data for pIR (Y1162/Y1163)/IR and pAkt (S473)/Akt and presented as means ± SEM. (*) indicates significant difference between chow (Ctr.) and fructose diets. (#) indicates significant difference between fructose (Fruct.) and fructose with fish oil (Fruct + F. Oil) diets.

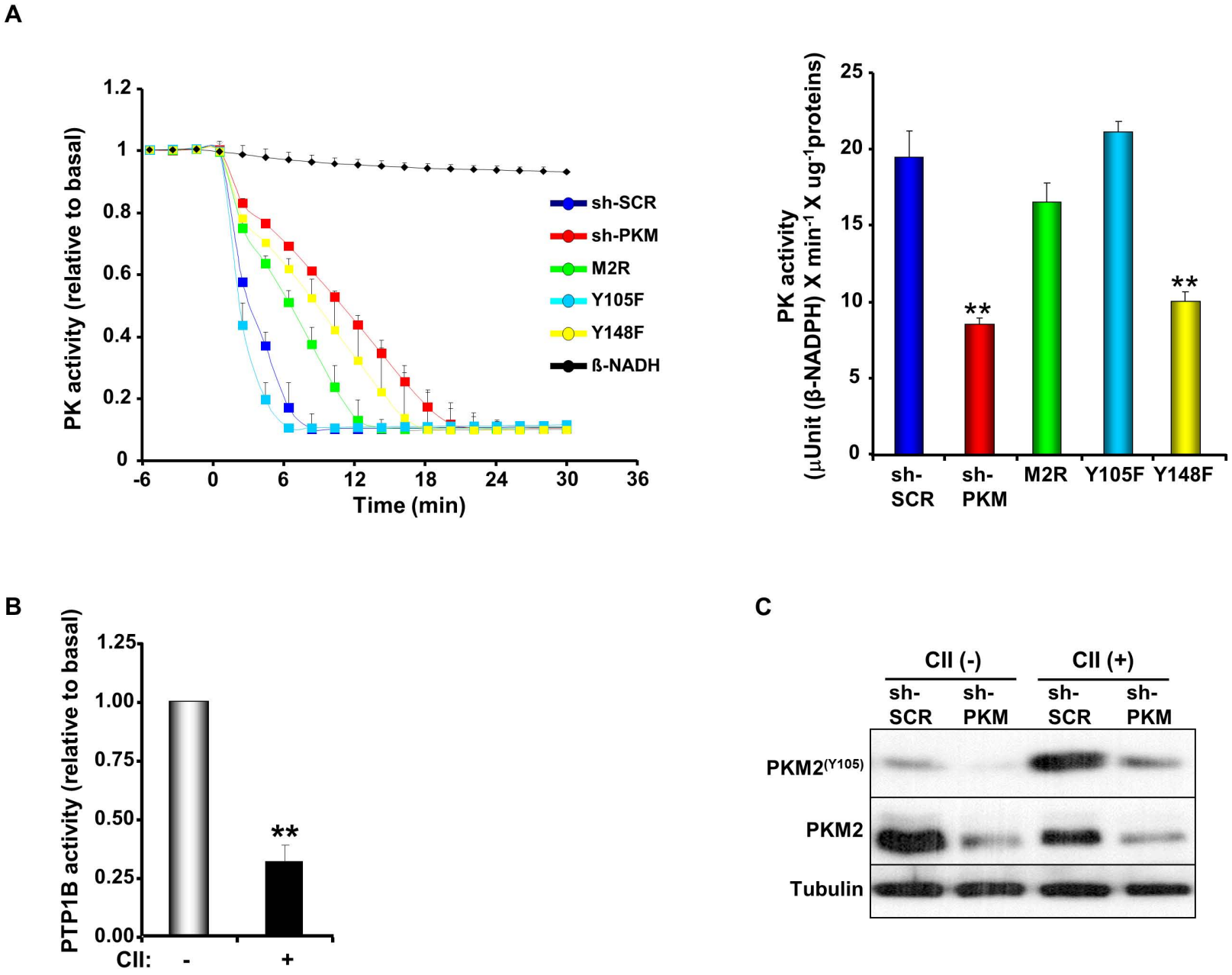
A
PK activity (relative to basal)
Time (min)
sh-SCR
sh-PKM
M2R
Y105F
Y148F
ß-NADH
PK activity (μUnit (β-NADPH) X min-1 X ug-1proteins)
sh-SCR
sh-PKM
M2R
Y105F
Y148F
B
PTP1B activity (relative to basal)
CII: - +
C
CII (-)
CII (+)
sh-SCR
sh-PKM
PKM2(Y105)
PKM2
Tubulin

Figure S1

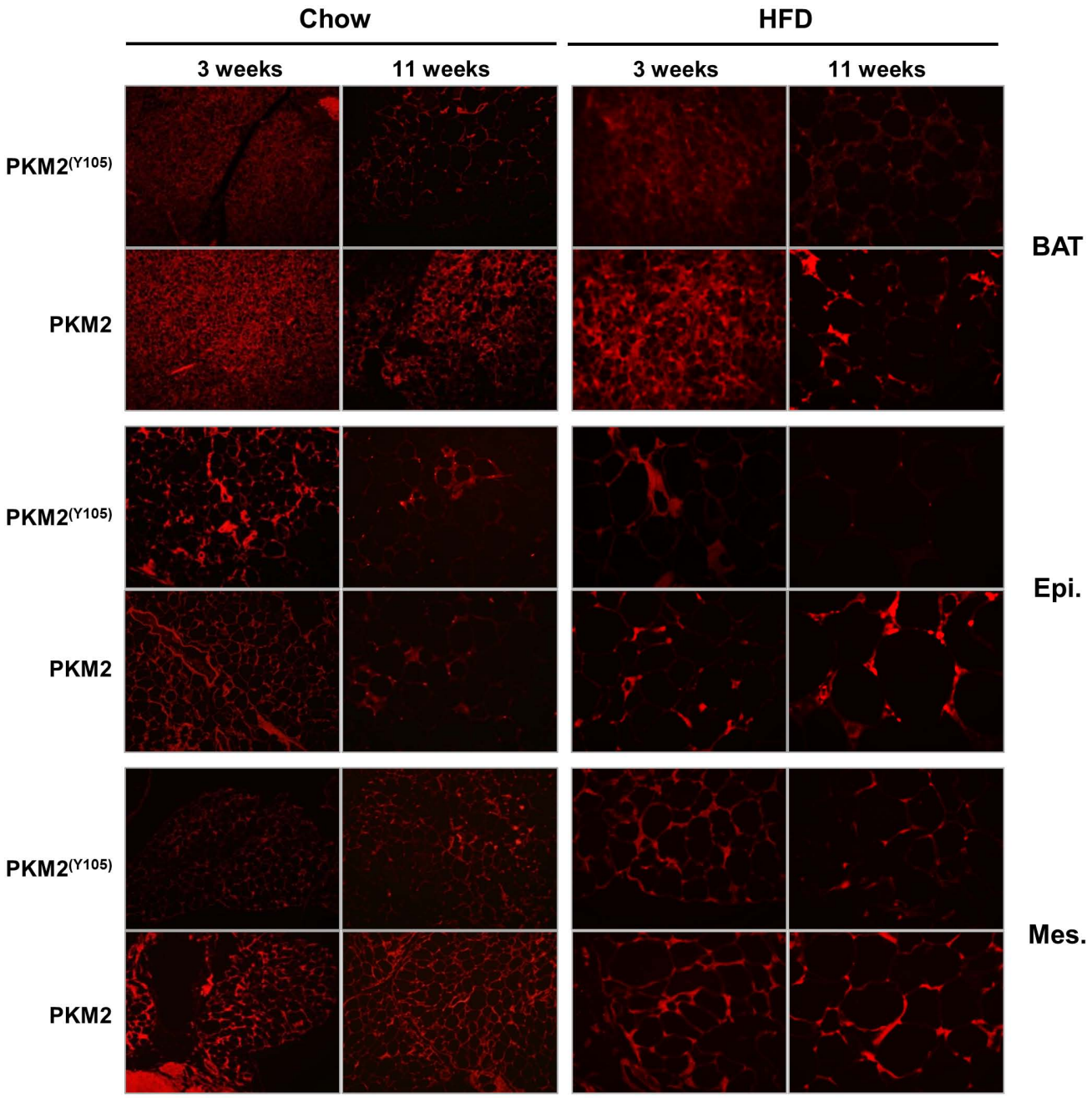
Chow
HFD
3 weeks
11 weeks
3 weeks
11 weeks
PKM2(Y105)
PKM2
BAT
PKM2(Y105)
PKM2
Epi.
PKM2(Y105)
PKM2
Mes.

Figure S2

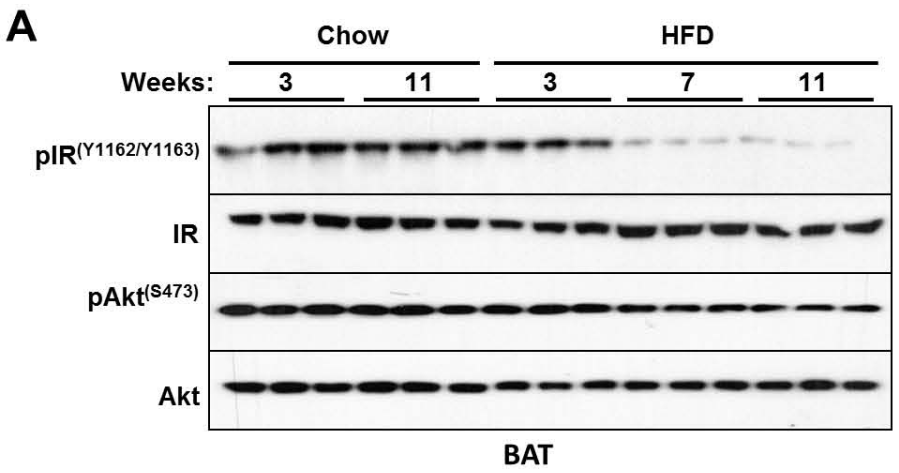
A
Chow
HFD
Weeks:
3
11
3
7
11
pIR(Y1162/Y1163)
IR
pAkt(S473)
Akt
BAT

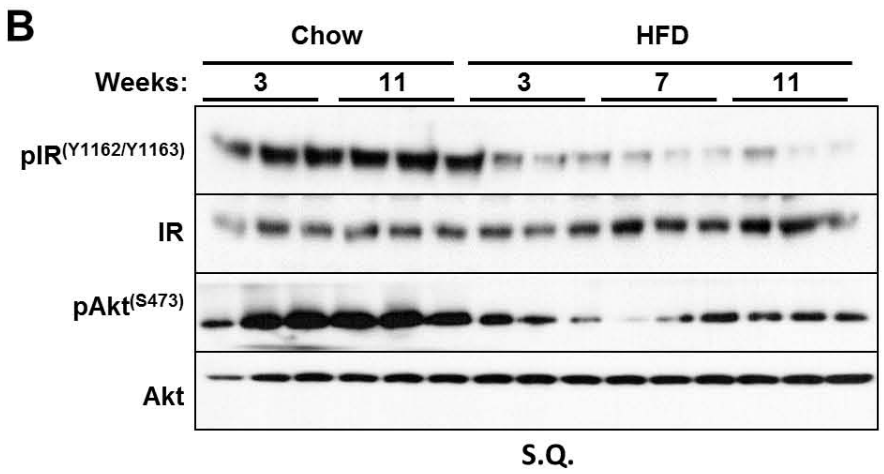
B
Chow
HFD
Weeks:
3
11
3
7
11
pIR(Y1162/Y1163)
IR
pAkt(S473)
Akt
S.Q.

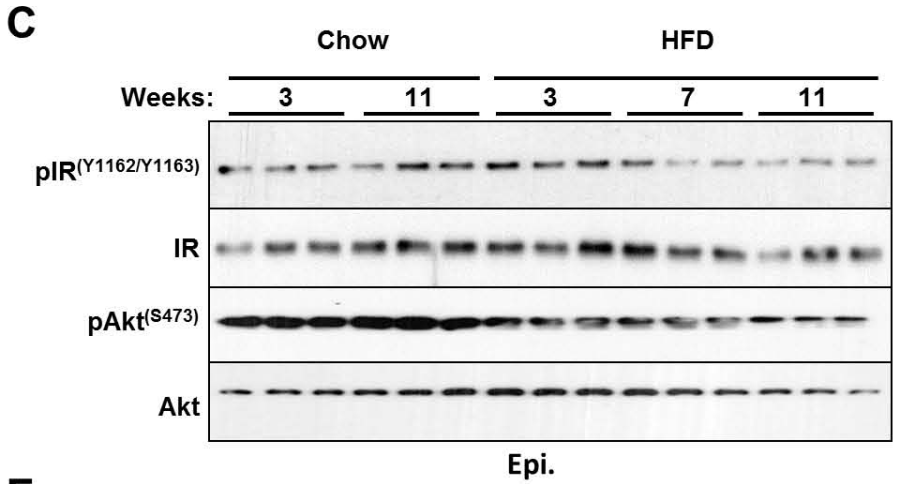
C
Chow
HFD
Weeks:
3
11
3
7
11
pIR(Y1162/Y1163)
IR
pAkt(S473)
Akt
Epi.

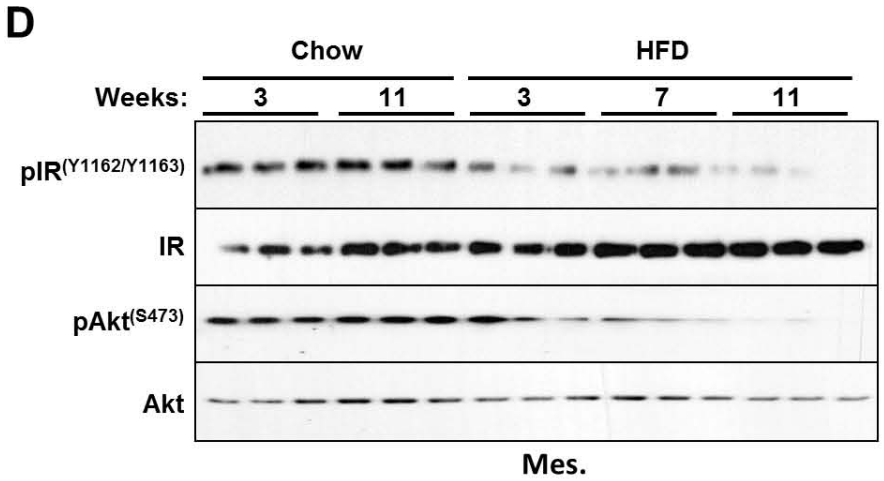
D
Chow
HFD
Weeks:
3
11
3
7
11
pIR(Y1162/Y1163)
IR
pAkt(S473)
Akt
Mes.

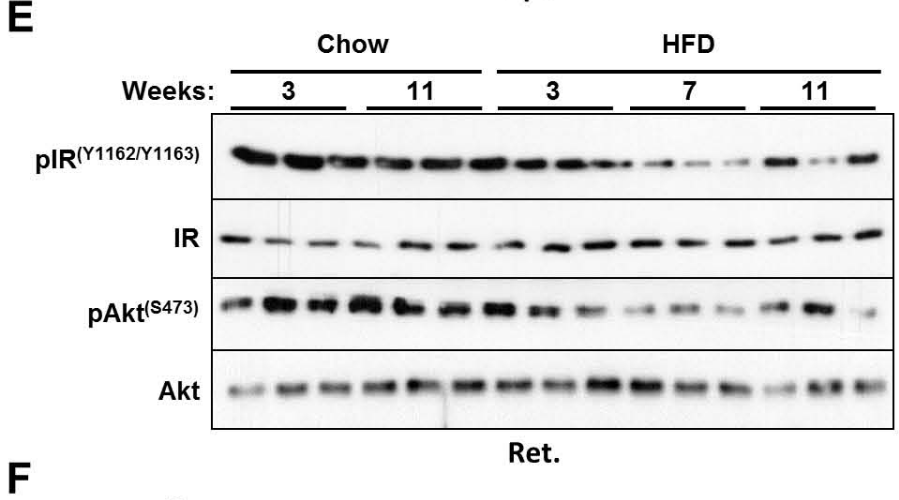
E
Chow
HFD
Weeks:
3
11
3
7
11
pIR(Y1162/Y1163)
IR
pAkt(S473)
Akt
Ret.

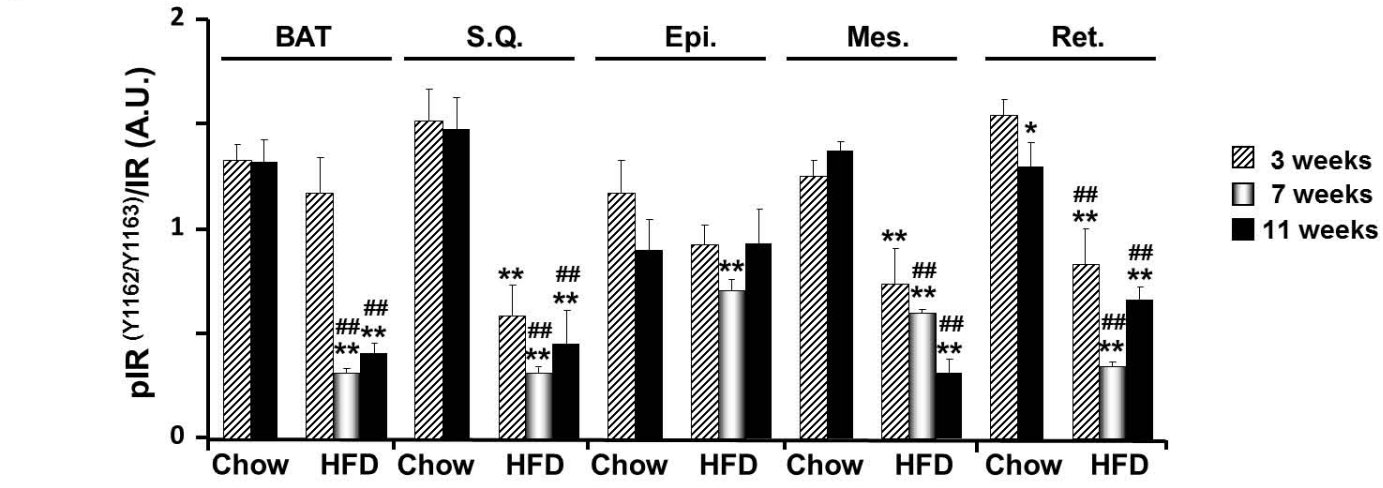
F
BAT
S.Q.
Epi.
Mes.
Ret.
pIR (Y1162/Y1163)/IR (A.U.)
2
1
0
Chow
HFD
3 weeks
7 weeks
11 weeks

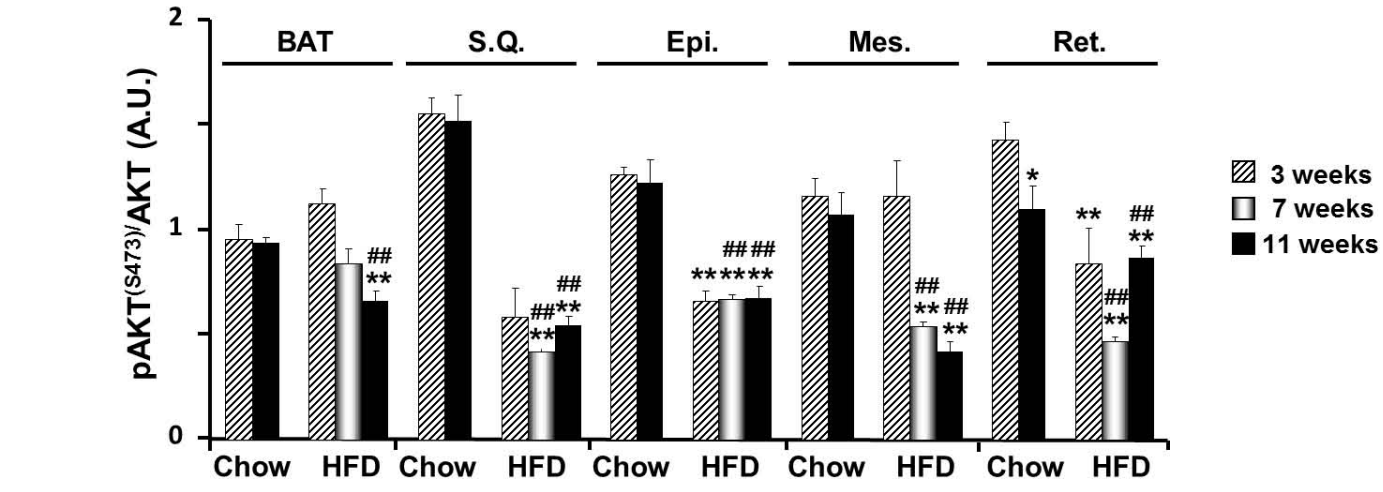
G
BAT
S.Q.
Epi.
Mes.
Ret.
pAKT(S473)/AKT (A.U.)
2
1
0
Chow
HFD
3 weeks
7 weeks
11 weeks

Figure S3

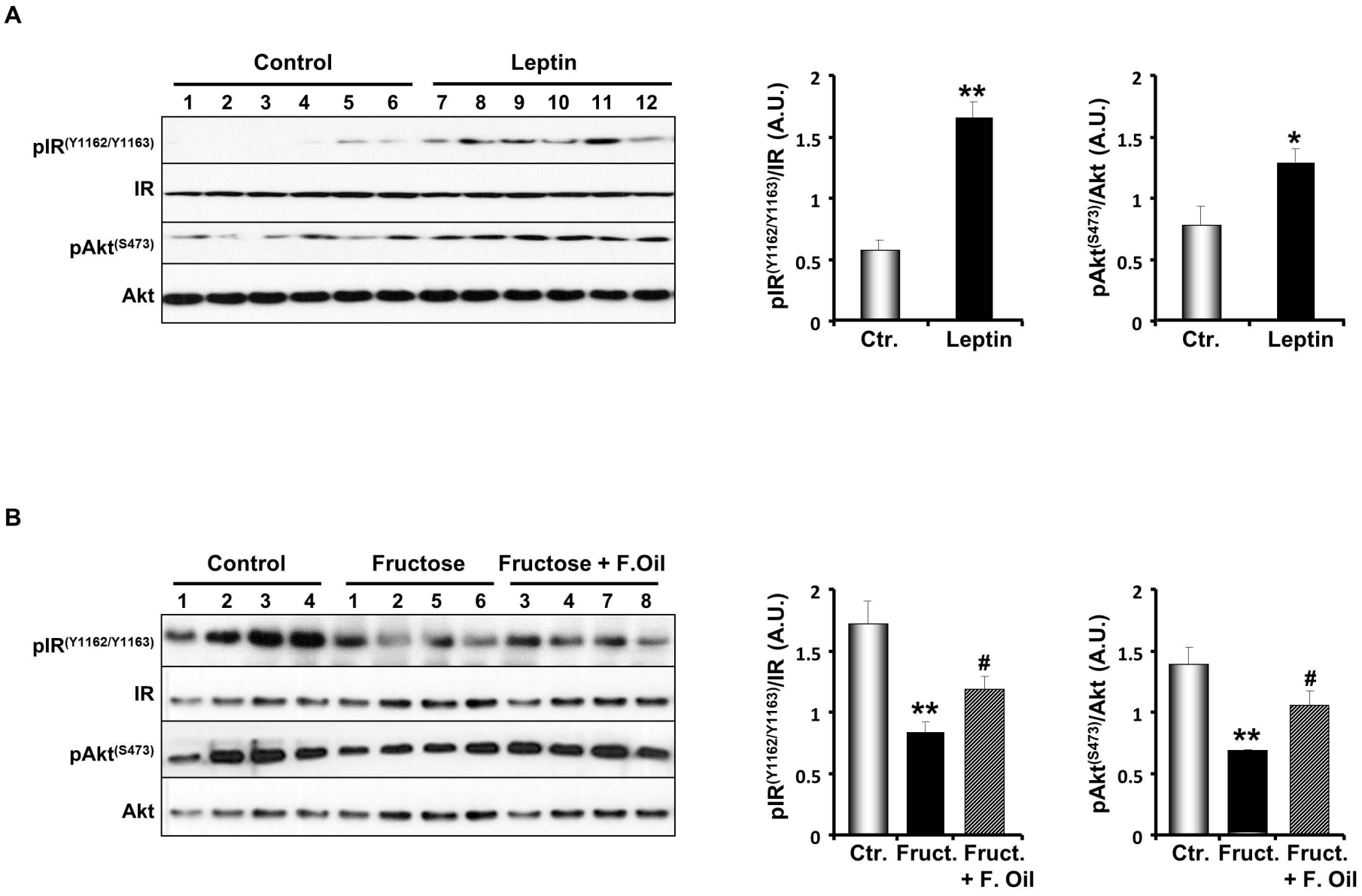
A
Control
Leptin
1 2 3 4 5 6 7 8 9 10 11 12
pIR(Y1162/Y1163)
IR
pAkt(S473)
Akt
pIR(Y1162/Y1163)/IR (A.U.)
**
Ctr.
Leptin
pAkt(S473)/Akt (A.U.)
*
Ctr.
Leptin
B
Control
Fructose
Fructose + F.Oil
1 2 3 4 1 2 5 6 3 4 7 8
pIR(Y1162/Y1163)
IR
pAkt(S473)
Akt
pIR(Y1162/Y1163)/IR (A.U.)
**
#
Ctr. Fruct. Fruct. + F. Oil
pAkt(S473)/Akt (A.U.)
**
#
Ctr. Fruct. Fruct. + F. Oil

Figure S4